



Deposited via The University of Sheffield.

White Rose Research Online URL for this paper:

<https://eprints.whiterose.ac.uk/id/eprint/215564/>

Version: Published Version

Article:

Aad, G., Aakvaag, E., Abbott, B. et al. (2024) Search for nearly mass-degenerate Higgsinos using low-momentum mildly displaced tracks in pp collisions at $s = 13\text{TeV}$ with the ATLAS detector. *Physical Review Letters*, 132. 221801. ISSN: 0031-9007

<https://doi.org/10.1103/physrevlett.132.221801>

Reuse

This article is distributed under the terms of the Creative Commons Attribution (CC BY) licence. This licence allows you to distribute, remix, tweak, and build upon the work, even commercially, as long as you credit the authors for the original work. More information and the full terms of the licence here:


<https://creativecommons.org/licenses/>

Takedown

If you consider content in White Rose Research Online to be in breach of UK law, please notify us by emailing eprints@whiterose.ac.uk including the URL of the record and the reason for the withdrawal request.

Search for Nearly Mass-Degenerate Higgsinos Using Low-Momentum Mildly Displaced Tracks in pp Collisions at $\sqrt{s} = 13$ TeV with the ATLAS Detector

G. Aad *et al.**
(ATLAS Collaboration)

 (Received 26 January 2024; accepted 10 April 2024; published 30 May 2024)

Higgsinos with masses near the electroweak scale can solve the hierarchy problem and provide a dark matter candidate, while detecting them at the LHC remains challenging if their mass splitting is $\mathcal{O}(1$ GeV). This Letter presents a novel search for nearly mass-degenerate Higgsinos in events with an energetic jet, missing transverse momentum, and a low-momentum track with a significant transverse impact parameter using 140 fb^{-1} of proton-proton collision data at $\sqrt{s} = 13$ TeV collected by the ATLAS experiment. For the first time since LEP, a range of mass splittings between the lightest charged and neutral Higgsinos from 0.3 to 0.9 GeV is excluded at 95% confidence level, with a maximum reach of approximately 170 GeV in the Higgsino mass.

DOI: [10.1103/PhysRevLett.132.221801](https://doi.org/10.1103/PhysRevLett.132.221801)

The *natural* solution from supersymmetry [1–6] to the hierarchy problem [7,8] provides a strong motivation to search for light Higgsinos, the fermionic partners of the Higgs bosons. Since the Higgsino mass is connected to the electroweak symmetry breaking scale in the minimal supersymmetric standard model (MSSM) [9,10], it is generally favored to be near the electroweak scale [$\mathcal{O}(100$ GeV)] in this framework. This light Higgsino scenario is also appealing because it provides a viable dark matter (DM) candidate if R parity [11] is conserved, and a neutral Higgsino is the stable lightest supersymmetric particle with a mass below 1.1 TeV [12,13]. These considerations indicate that Higgsinos may be within the mass reach of the Large Hadron Collider (LHC), and the direct production of Higgsinos has been a key probe for the search program.

The Higgsino phenomenology highly depends on their mass hierarchy with respect to the wino and bino, the fermionic partners of the $SU(2)_L$ and $U(1)_Y$ gauge boson in the standard model (SM). In the MSSM, the Higgsino (\tilde{H}) and wino (\tilde{W}), and bino (\tilde{B}) fields, whose masses are characterized by the parameters μ , M_1 , and M_2 , respectively, undergo kinetic mixing as the result of the electroweak symmetry breaking, yielding charged ($\tilde{\chi}_1^\pm, \tilde{\chi}_2^\pm$) and neutral ($\tilde{\chi}_1^0, \tilde{\chi}_2^0, \tilde{\chi}_3^0, \tilde{\chi}_4^0$) mass eigenstates, where the order of the subscripts indicates increasing mass. In the case where $|\mu| \ll |M_1|, |M_2|$, the lightest charged and two neutral

Higgsino-like eigenstates form a nearly mass-degenerate triplet of Higgsino-like mass eigenstates ($\tilde{\chi}_1^\pm, \tilde{\chi}_2^0, \tilde{\chi}_1^0$), collectively referred to as Higgsinos in this Letter. In the pure Higgsino limit where the bino and wino are decoupled in mass, $\min(|M_1|, |M_2|) > \mathcal{O}(10$ TeV), radiative corrections induce a small mass splitting [$\Delta m(\tilde{\chi}_1^\pm, \tilde{\chi}_1^0) \approx 250$ – 400 MeV [14]] between the Higgsinos that gives the $\tilde{\chi}_1^\pm$ a long enough lifetime to produce the disappearing track signature in the detector, as exploited by existing searches [15–18]. On the other hand, mass splittings larger than a few GeV are possible when either the bino or wino states are light, $\min(|M_1|, |M_2|) < \mathcal{O}(1$ TeV), enabling low-momentum prompt lepton searches to target the $\tilde{\chi}_2^0 \rightarrow Z^* \tilde{\chi}_1^0 \rightarrow \ell^+ \ell^- \tilde{\chi}_1^0$ decay and provide constraints down to $\Delta m(\tilde{\chi}_2^0, \tilde{\chi}_1^0) \approx 2$ GeV [19–21]. However, a distinct sensitivity gap remains for $\Delta m(\tilde{\chi}_1^\pm, \tilde{\chi}_1^0) \approx 0.3$ – 1 GeV, where the strongest constraints are still set by the LEP experiments [22]. Importantly, this mass-splitting range is challenging for direct DM detection experiments due to the vanishing DM-nuclei coupling [23], while the $\Delta m(\tilde{\chi}_2^0, \tilde{\chi}_1^0) > 2$ GeV and pure Higgsino scenarios are highly constrained by those searches [14]. This Letter reports a new search by the ATLAS [24] experiment [25] to address this sensitivity gap. Following the proposal in Ref. [23] and described in detail below, the search identifies low-momentum charged particles that are consistent with the decay products of a $\tilde{\chi}_1^\pm$ that has a discernible flight length from the proton-proton (pp) collision point.

For the mass splitting of interest of $\Delta m(\tilde{\chi}_1^\pm, \tilde{\chi}_1^0) \approx 0.3$ – 1 GeV, the decay flight length of $\tilde{\chi}_1^\pm$ can reach $\mathcal{O}(0.1$ – 1 mm). Charged decay particles from $\tilde{\chi}_1^\pm$, dominated by charged pions, have a transverse momentum (p_T) of a few GeV, offering a reasonable reconstruction efficiency. The transverse impact parameter d_0 , with its

*Full author list given at the end of the Letter.

Published by the American Physical Society under the terms of the [Creative Commons Attribution 4.0 International license](https://creativecommons.org/licenses/by/4.0/). Further distribution of this work must maintain attribution to the author(s) and the published article's title, journal citation, and DOI. Funded by SCOAP³.

resolution $\sigma(d_0)$, is the distance of closest approach of the charged particle trajectory in the transverse (x - y) plane with respect to the centroid of the pp collision of interest. Since the displacement of the $\tilde{\chi}_1^\pm$ decay position from the pp collision point is correlated to d_0 , the transverse impact parameter significance, $S(d_0) = |d_0|/\sigma(d_0)$, can be the most distinctive discriminant to identify the decay of $\tilde{\chi}_1^\pm$ together with an adequate requirement of p_T . The $\tilde{\chi}_1^\pm$ flight length is sufficiently short so that most of the decay charged particles are expected to pass through the innermost tracking layer. Satisfying such a decay condition with sufficiently large $S(d_0)$ is referred to as ‘‘mildly displaced’’ in this Letter. The production of a Higgsino-pair system with initial-state radiation (ISR) can be used to trigger the event based on missing transverse momentum (denoted as $\mathbf{p}_T^{\text{miss}}$ along with its magnitude E_T^{miss}). Moreover, the additional Lorentz boost by the ISR recoil enhances both p_T and $S(d_0)$, so that more decay charged particles get mildly displaced, which increases the sensitivity to even smaller mass-splitting values. While the conventional ‘‘monojet’’ searches [26,27] that probe this ISR event topology for generic DM production at the LHC do not provide significant sensitivity to Higgsino production due to the overwhelming SM background, the inclusion of a displaced track requirement allows for a significant reduction of these backgrounds, which allows the exploration of this range of mass-splitting values for the first time since LEP. This search uses the pp collision data collected at the LHC during 2015–2018 at a center-of-mass energy of $\sqrt{s} = 13$ TeV, corresponding to an integrated luminosity of 140 fb^{-1} .

An example signal diagram of the targeted signature is shown in Fig. 1. The same R -parity conserving Higgsino simplified model is considered as in Refs. [19,20] where the mass of the $\tilde{\chi}_1^\pm$ is halfway between that of the $\tilde{\chi}_2^0$ and the $\tilde{\chi}_1^0$, i.e., $m(\tilde{\chi}_2^0) - m(\tilde{\chi}_1^\pm) = m(\tilde{\chi}_1^\pm) - m(\tilde{\chi}_1^0)$. The Higgsino-pair production modes considered are $\tilde{\chi}_1^+\tilde{\chi}_1^-$, $\tilde{\chi}_1^\pm\tilde{\chi}_1^0$, $\tilde{\chi}_1^\pm\tilde{\chi}_2^0$,

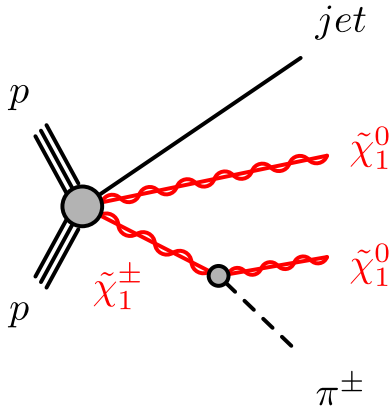


FIG. 1. Example signal diagram for the targeted signature featuring a jet from initial-state radiation. For illustration, the $\tilde{\chi}_1^\pm\tilde{\chi}_1^0$ process is shown, while the production of $\tilde{\chi}_1^+\tilde{\chi}_1^-$, $\tilde{\chi}_1^\pm\tilde{\chi}_2^0$, and $\tilde{\chi}_2^0\tilde{\chi}_1^0$ is considered in the search as well.

and $\tilde{\chi}_2^0\tilde{\chi}_1^0$. The largest branching ratio of $\tilde{\chi}_1^\pm$ ($\tilde{\chi}_2^0$) decays is to a single π^\pm (π^0) when $\Delta m(\tilde{\chi}_1^\pm, \tilde{\chi}_1^0) = 0.3$ – 1 GeV [28]; about 80% of $\tilde{\chi}_1^\pm$ decays to $\pi^\pm\tilde{\chi}_1^0$ with $\Delta m(\tilde{\chi}_1^\pm, \tilde{\chi}_1^0) = 0.5$ GeV, and about 70% of $\tilde{\chi}_2^0$ decays to $\pi^0\tilde{\chi}_1^0$ with $\Delta m(\tilde{\chi}_2^0, \tilde{\chi}_1^0) = 0.5$ GeV. The identified displaced track in signal events therefore typically corresponds to a π^\pm from a $\tilde{\chi}_1^\pm$ decay, but a small fraction can also arise from $\tilde{\chi}_1^\pm \rightarrow e\nu\tilde{\chi}_1^0$, $\tilde{\chi}_1^\pm \rightarrow \mu\nu\tilde{\chi}_1^0$, $\tilde{\chi}_2^0 \rightarrow e^+e^-\tilde{\chi}_1^0$, $\tilde{\chi}_2^0 \rightarrow \mu^+\mu^-\tilde{\chi}_1^0$, and $\tilde{\chi}_2^0 \rightarrow \pi^+\pi^-\tilde{\chi}_1^0$ decays; all are taken into account as signal in the analysis.

The ATLAS experiment is a multipurpose particle detector with a forward-backward symmetric cylindrical geometry and nearly 4π coverage in solid angle. It consists of an inner tracking detector (ID) surrounded by a superconducting solenoid, sampling electromagnetic (EM) and hadronic calorimeters, and a muon spectrometer (MS) with three toroidal superconducting magnets. Charged particle tracks are reconstructed using the hits in the ID and are required to have $p_T > 500$ MeV. For tracks with $p_T = 2$ GeV, the intrinsic resolution on d_0 is approximately 0.05 mm, which improves to 0.03 mm at $p_T = 5$ GeV and 0.01 mm at $p_T > 10$ GeV [29]. A two-level trigger system is used to select events for storage. The events in the main dataset used in this analysis relied on the E_T^{miss} trigger [30], while the auxiliary dataset for the background estimation and validation was collected using the single-electron [31] or single-photon triggers [31]. An extensive software suite [32] is used in data simulation, in the reconstruction and analysis of real and simulated data, in detector operations, and in the trigger and data acquisition systems of the experiment.

The pp interaction vertex with the highest p_T^2 sum of associated tracks is selected as the hard-scatter vertex of interest. Hadronic jets are reconstructed from particle-flow objects [33] calibrated at the EM scale using the anti- k_r algorithm [34,35] with a radius parameter of $R = 0.4$. Jets with $p_T > 20$ GeV and $|\eta| < 2.8$ are considered in the analysis. To suppress the contribution from additional pp collisions in the same and neighboring bunch crossings (‘‘pileup’’), jets with $p_T < 60$ GeV and $|\eta| < 2.5$ are required to pass the ‘‘tight’’ working point of the jet vertex tagger [36].

Electrons, muons, and photons are reconstructed and selected mainly to define the events used for the background estimation and validation. Electrons are reconstructed from energy deposits in the EM calorimeter associated with tracks found in the ID. Muons are reconstructed by combining tracks reconstructed in the ID with tracks or track segments found in the MS. Electrons (muons) must have $p_T > 4.5(3)$ GeV, be reconstructed within $|\eta| < 2.47(2.7)$, and satisfy the tight [37] (medium [38]) identification criterion. To ensure that selected electrons and muons (collectively referred to as

leptons in this Letter and denoted by ℓ) originate from the selected hard-scatter vertex, their tracks are required to fulfill $|z_0 \sin \theta| < 0.5$ mm, where z_0 is the longitudinal impact parameter. Photons are reconstructed as EM clusters with either no matching ID track or with a matching conversion vertex from e^+e^- pairs in the ID material [37]. Photon candidates with $p_T > 25$ GeV and $|\eta| < 2.37$ passing the tight identification criterion [37] are selected.

To prevent the reconstruction of a single particle as multiple objects, an overlap removal procedure described in Ref. [39] is applied to the leptons, photons, and jets. The E_T^{miss} is calculated as the magnitude of the negative vectorial sum of the transverse momenta of all leptons, photons, and jets calibrated to their respective energy scales and an additional soft term constructed from tracks originating from the hard-scatter vertex, but not associated with any of the reconstructed objects [40]. Jets in the forward direction (up to $|\eta| < 4.5$) are also considered in the E_T^{miss} calculation.

Finally, the low- p_T charged track from the $\tilde{\chi}_1^\pm$ or $\tilde{\chi}_2^0$ decays, referred to as the signal candidate track, is defined as an ID track associated with the hard-scatter vertex that fulfills: $2 < p_T < 5$ GeV, $|\eta| < 1.5$, $|d_0| < 10$ mm, $|z_0 \sin \theta| < 3$ mm, and the ‘‘tight primary’’ track selection criteria defined in Ref. [41]. The loose requirement on the track $|d_0|$ retains efficiency for charged particles with long lifetimes, while the tight primary requirement ensures high quality tracks based on the number of hits in the silicon detectors of the ID system. A signal candidate track must also have a measurement in the first layer of the ID at a radius of approximately 33 mm and not be associated with any secondary K_S^0 or Λ decay vertices as identified by an algorithm optimized to reconstruct two-body $V0$ decays [42,43]. An isolation requirement is applied such that no other tight primary tracks satisfying $p_T > 1$ GeV, $|d_0| < 10$ mm, and $|z_0 \sin \theta| < 3$ mm are allowed within an angular distance of $\Delta R < 0.4$ with respect to the signal candidate track. The signal candidate track needs to be aligned with the $\mathbf{p}_T^{\text{miss}}$ by requiring $\Delta\phi(\text{track}, \mathbf{p}_T^{\text{miss}}) < 0.4$, reflecting the targeted event topology in which the Higgsinos are collimated due to the transverse boost by the recoiling ISR jet. If multiple tracks pass this selection, the track with the highest $S(d_0)$ is selected as the signal candidate track.

Monte Carlo (MC) simulations are used to model the Higgsino signals and the SM backgrounds, where the generation of all simulated event samples includes the effect of multiple pp interactions per bunch crossing, as well as the effect on the detector response due to interactions from bunch crossings before or after the one containing the hard interaction. Details about the event simulation configurations used can be found in Appendix A. For signal samples the lifetime and branching ratios of the $\tilde{\chi}_1^\pm$ and $\tilde{\chi}_2^0$ are calculated following the prescription described in Ref. [28] and propagated to the

simulation of their decays during the event generation. The signal cross sections are computed at next-to-leading order (NLO) in the strong coupling constant, adding the resummation of soft-gluon emission at next-to-leading-logarithm accuracy [44–49]. The PDF4LHC15_mc parton distribution function (PDF) set is used following the recommendations in Ref. [50]. The production cross section is 3.95 pb for $m(\tilde{\chi}_2^0, \tilde{\chi}_1^\pm, \tilde{\chi}_1^0) = (151, 150.5, 150)$ GeV with all of the production modes $(\tilde{\chi}_1^+ \tilde{\chi}_1^-, \tilde{\chi}_1^\pm \tilde{\chi}_{1,2}^0, \tilde{\chi}_2^0 \tilde{\chi}_1^0)$ included.

The dominant SM background originates from events with a leptonically decaying $W(\rightarrow \ell\nu/\tau\nu)$ or $Z(\rightarrow \nu\nu/\tau\tau)$ boson associated with jets, referred to as $W + \text{jets}$ and $Z + \text{jets}$, respectively. Other background processes include diboson $t\bar{t}$ and single top-quark production. The production of QCD multijet, triboson, and other rare processes including top quarks were found to be negligible.

The signal region (SR) is defined by selecting events that have no leptons or photons after the E_T^{miss} trigger requirement. A set of event cleaning criteria is applied [51], including a veto of events with cosmic muons or muons with poor p_T determination. The events must also contain at least one jet with $p_T > 250$ GeV and $|\eta| < 2.4$, but no more than four jets to suppress the $t\bar{t}$ background. To ensure the removal of beam-induced background, events are rejected if the highest p_T jet has an anomalous energy profile in the calorimeter that fails the tight cleaning criteria [52]. The azimuthal angular separation between $\mathbf{p}_T^{\text{miss}}$ and all jets must satisfy $\Delta\phi(j, \mathbf{p}_T^{\text{miss}}) > 0.4$ to suppress the QCD multijet background. Additionally, events are required to have $E_T^{\text{miss}} > 600$ GeV in order to reject the bulk of the SM backgrounds, primarily from $W/Z + \text{jets}$ production. This offline E_T^{miss} requirement is well above 200 GeV, where the E_T^{miss} trigger is already found to be fully efficient. Finally, the presence of a signal candidate track with a transverse displacement significance of $S(d_0) > 8$ is required. The $S(d_0)$ selection efficiency is approximately 40% for tracks originating from Higgsino decays in a signal MC sample with $\Delta m(\tilde{\chi}_1^\pm, \tilde{\chi}_1^0) = 0.5$ GeV. The SR is split into two bins labeled SR-Low [$8 < S(d_0) < 20$] and SR-High [$S(d_0) > 20$] to maintain sensitivity to a range of mass splittings. With all of the selection criteria applied, the acceptance times efficiency in the union of SR-Low and SR-High is roughly 2.1×10^{-4} for the Higgsino signal model with $m(\tilde{\chi}_1^0) = 150$ and $\Delta m(\tilde{\chi}_1^\pm, \tilde{\chi}_1^0) = 0.5$ GeV.

The leading SM background is $W(\rightarrow \tau\nu) + \text{jets}$ production where a pion or lepton from a low- p_T τ -lepton decay is tagged as the signal candidate track. This background is referred to as the ‘‘ τ track’’ background. Such tracks tend to exhibit a harder p_T spectrum compared to the signals of interest, and their contribution to the SR is largely reduced by the track $p_T < 5$ GeV requirement. To estimate this background, a partially data-driven method is used where the MC sample is normalized to control regions (CRs) with

higher track p_T (8–20 GeV) with respect to the SR. A CR with exactly zero (one) leptons is used to constrain the hadronic (leptonic) τ decay background yield. Both τ track background MC samples share the same normalization factor. A test was performed in which separate normalization factors were derived for the hadronic and leptonic τ decay backgrounds, resulting in a consistent prediction of their event yields in the SR bins compared to the use of a single normalization factor.

The subleading SM background is $W/Z + \text{jet}$ events where the signal candidate tracks arise from hadrons with measurably long lifetimes (e.g., Λ , K_S^0) in pileup jets or the underlying event, referred to as the “QCD track” background. These tracks tend to dominate at low p_T , motivating the $p_T > 2$ GeV requirement for signal tracks that significantly reduces their contribution to the SR. A fully data-driven method is employed to estimate this background. First, the shape of the $S(d_0)$ distribution is extracted from the data events in a control region with exactly one muon (CR-1 μ), which is dominated by $W(\rightarrow \mu\nu) + \text{jets}$. This sample is then normalized to the data in a low- $S(d_0)$ control region (CR-0 ℓ) to obtain the estimate in the SR, where CR-0 ℓ is defined to be adjacent to the SR by inverting the $S(d_0)$ selection [i.e., $S(d_0) < 8$]. This method relies on the fact that the shape of the $S(d_0)$ distribution is dictated by the breakdown of the hadron components in the pileup jets or underlying events, which do not strongly depend on the details of the hard collision process. Control region CR-1 μ has the same selection as the SR, except that exactly one muon is required and that $p_T^{\text{recoil}} > 300$ GeV is applied instead of $E_T^{\text{miss}} > 600$, where $p_T^{\text{recoil}} = |\mathbf{p}_T(\mu) + \mathbf{p}_T^{\text{miss}}|$ is the proxy for the p_T of the W boson. The loosened selection allows roughly a factor of 30 increase in the data yield in the CR. Contributions from SM processes other than $W(\rightarrow \mu\nu) + \text{jets}$ are subtracted when extracting the shape of the $S(d_0)$ distribution.

Backgrounds other than the τ track and the QCD track background are minor and are estimated using the MC simulation.

The background modeling is tested by comparing the estimates and the data in dedicated validation regions (VRs). The τ track background estimate is validated in regions with an intermediate track p_T (5–8 GeV) adjacent to the SR (2–5 GeV), with a shifted E_T^{miss} requirement of $300 < E_T^{\text{miss}} < 400$ GeV to increase the data yield and to suppress signal contamination. For the QCD track background estimate, the validity of the $S(d_0)$ shape as extracted from $W(\rightarrow \mu\nu) + \text{jet}$ events is verified in dedicated VRs defined by requiring either one electron, two leptons, or one photon, which are dominated by $W(\rightarrow e\nu) + \text{jet}$, $Z(\rightarrow \ell\ell) + \text{jet}$, and $\gamma + \text{jet}$ production, respectively. Here, the signal candidate tracks have an origin similar to that of QCD track events in CR-1 μ and the SR. An additional VR populated with both the τ track and QCD track backgrounds is defined near the SR to test the

estimate of both components (VR-0 ℓ -low E_T^{miss}). This VR is defined by shifting the E_T^{miss} selection with respect to the SR to $300 < E_T^{\text{miss}} < 400$ GeV. A more detailed description of the VRs is given in Appendix B, and schematic illustrations of the region layout can be found in the Supplemental Material [53] of this Letter.

To obtain the final background estimates, the extraction and the application of the $S(d_0)$ shape for the QCD track background and the normalization of the τ track background are performed via a simultaneous profile log-likelihood fit [54] including all CRs. SRs and VRs are not included in the fit as constraints to estimate the backgrounds. Systematic uncertainties are implemented in the fit as nuisance parameters constrained by Gaussian probability density functions. Correlations between systematic uncertainties arising from common sources are maintained across processes and regions. Instrumental and theoretical uncertainties are assigned on the modeling of signals and backgrounds except for the QCD track background. The instrumental uncertainties include those on lepton trigger, reconstruction, and identification efficiencies [38,55], lepton energy scale and resolution [38,56], jet energy scale and resolution [57], jet vertex tagging [58], modeling of E_T^{miss} [40] and pileup, and integrated luminosity [59]. Theoretical uncertainties include the cross section uncertainties and the shape uncertainties due to the renormalization and

TABLE I. Number of expected and observed data events in the SR (top) and the model-independent upper limits obtained from their consistency (bottom). The symbol τ_ℓ (τ_h) refers to fully leptonic (hadron-involved) τ decays. The “others” category includes contributions from minor background processes including $t\bar{t}$, single top, and diboson. The individual uncertainties can be correlated and do not necessarily sum up in quadrature to the total uncertainty. The uncertainty associated with the expected number of events includes the systematic uncertainty and the statistical uncertainty due to the limit data sample size in the CRs. The bottom section shows the observed 95% CL upper limits on the visible cross section ($\langle\epsilon\sigma\rangle_{\text{obs}}^{95}$) and on the number of generic signal events (S_{obs}^{95}), as well as the expected limit (S_{exp}^{95}) given the expected number (and $\pm 1\sigma$ deviations from the expectation) of background events.

	SR-Low	SR-High
Observed data	35	15
SM prediction	37 ± 4	14.8 ± 2.0
QCD track	14.0 ± 1.7	10.0 ± 1.6
$W(\rightarrow \tau_\ell\nu) + \text{jets}$	9.6 ± 1.6	2.0 ± 0.6
$W(\rightarrow \tau_h\nu) + \text{jets}$	10.6 ± 2.0	1.9 ± 0.8
Others	3.2 ± 0.7	0.8 ± 0.4
$\langle\epsilon\sigma\rangle_{\text{obs}}^{95}$ (fb)	0.10	0.07
S_{obs}^{95}	13.5	9.9
S_{exp}^{95}	$15.1^{+6.3}_{-4.2}$	$9.6^{+4.4}_{-2.8}$

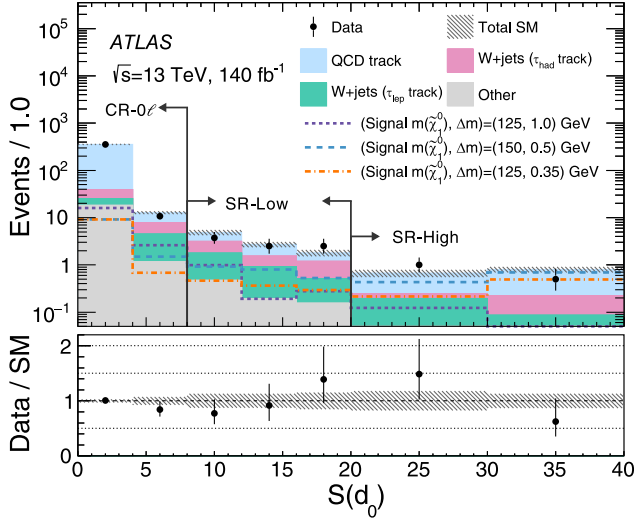


FIG. 2. Postfit $S(d_0)$ distribution in, and near, the SR and the adjacent control region CR-0 ℓ . The selection criterion on the variable shown by each plot is removed, while the arrow indicates the cut value to define the region. The SM background expectation is shown as a histogram stack, and a few representative signal models are overlaid. The last bin includes the overflow. The hatched band indicates the uncertainty on the mean value of the SM background expectation, while the error bars on the black dots represent the Poisson error associated with the event yields.

factorization scales [60], PDFs [50], and parton showering. For the data-driven estimate on the QCD track background, uncertainties of 5% and 10% are assigned to SR-Low and SR-High, respectively, to account for any potential $S(d_0)$ shape difference between CR-1 μ and the SR and VRs due to the varying physics processes involved and kinematic selections, as evaluated in MC simulation. The fit also includes the systematic uncertainties due to limited MC simulation sample sizes and the data sample size in the CRs, which are the dominant contributions among all systematic uncertainties in the SR and VRs. The background estimate is found to agree well with the observed data in all of the VRs within the uncertainty.

The numbers of observed events in each SR bin are summarized in Table I, along with the SM background predictions. The MC normalization factor for the τ track background is found to be 1.1 ± 0.1 , derived from a fit under the background-only hypothesis. The postfit $S(d_0)$ distribution in the SR is shown in Fig. 2, where no significant deviation from the expectation is observed. The absence of a data excess is translated into exclusion limits at 95% confidence level (CL) on the Higgsino simplified model using the CL_s prescription [61] employing the asymptotic formulas [54] for the profile likelihood ratio. The two SR bins are included as constraints in the fit for computing exclusion limits. Including the SRs has a negligible effect on the fitted background yields. The obtained expected and observed exclusion limits are shown in Fig. 3, where mass splittings in the range of

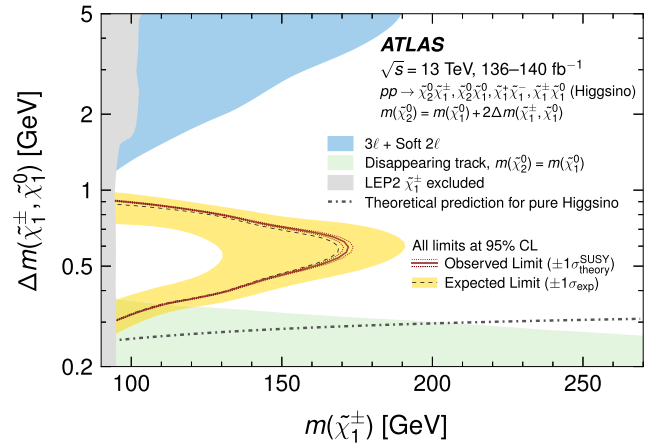


FIG. 3. Expected (dashed black line) and observed (solid red line) 95% CL exclusion limits on the Higgsino simplified model being considered. These are shown with $\pm 1\sigma_{\text{exp}}$ (yellow band), from experimental systematic and statistical uncertainties, and with $\pm 1\sigma_{\text{theory}}^{\text{SUSY}}$ (red dotted lines) from signal cross section uncertainties, respectively. The limits set by the latest ATLAS searches using the soft lepton [19,20] and disappearing track [16] signatures are illustrated by the blue and green regions, respectively, while the limit imposed by the LEP experiments [22] is shown in gray. The dot-dashed gray line indicates the predicted mass splitting for the pure Higgsino scenario [62].

$0.3 < \Delta m(\tilde{\chi}_1^\pm, \tilde{\chi}_1^0) < 0.9$ GeV are excluded for a given value of $m(\tilde{\chi}_1^\pm)$. The search sensitivity peaks at $\Delta m(\tilde{\chi}_1^\pm, \tilde{\chi}_1^0) = 0.6$ GeV, for which $m(\tilde{\chi}_1^\pm)$ is excluded up to approximately 170 GeV in $m(\tilde{\chi}_1^\pm)$. The model-independent upper limits and constraints on generic physics processes beyond the standard model are also derived. These limits, assuming no signal contamination in the CRs, are presented in Table I.

In conclusion, this Letter reports the results of a search for the pair production of nearly mass-degenerate Higgsinos using 140 fb^{-1} of pp collision data at $\sqrt{s} = 13$ TeV collected with the ATLAS detector at the LHC. A novel signature is explored for the first time in LHC searches. It features the use of a low- p_T displaced track to achieve sensitivity to a largely unconstrained region of the 0.3–1 GeV Higgsino mass-splitting parameter range, which is challenging to probe with direct DM search experiments. No excess above the SM expectation is observed and mass limits are set at 95% CL within a simplified Higgsino model, where Higgsino masses of up to about 170 GeV are excluded, exceeding the limit set by the LEP experiments for the first time. This result bridges a long-standing blind spot in the sensitivity of Higgsino searches and establishes prospects for a conclusive test of the natural supersymmetry scenario, which predicts an electroweak-scale Higgsino mass.

We thank CERN for the very successful operation of the LHC and its injectors, as well as the support staff at CERN

and at our institutions worldwide without whom ATLAS could not be operated efficiently. The crucial computing support from all WLCG partners is acknowledged gratefully, in particular, from CERN, the ATLAS Tier-1 facilities at TRIUMF/SFU (Canada), NDGF (Denmark, Norway, Sweden), CC-IN2P3 (France), KIT/GridKA (Germany), INFN-CNAF (Italy), NL-T1 (Netherlands), PIC (Spain), RAL (UK), and BNL (U.S.), the Tier-2 facilities worldwide, and large non-WLCG resource providers. Major contributors of computing resources are listed in Ref. [63]. We gratefully acknowledge the support of ANPCyT, Argentina; YerPhI, Armenia; ARC, Australia; BMWFW and FWF, Austria; ANAS, Azerbaijan; CNPq and FAPESP, Brazil; NSERC, NRC, and CFI, Canada; CERN; ANID, Chile; CAS, MOST, and NSFC, China; Minciencias, Colombia; MEYS CR, Czech Republic; DNRF and DNSRC, Denmark; IN2P3-CNRS and CEA-DRF/IRFU, France; SRNSFG, Georgia; BMBF, HGF, and MPG, Germany; GSRI, Greece; RGC and Hong Kong SAR, China; ISF and Benozio Center, Israel; INFN, Italy; MEXT and JSPS, Japan; CNRST, Morocco; NWO, Netherlands; RCN, Norway; MEiN, Poland; FCT, Portugal; MNE/IFA, Romania; MESTD, Serbia; MSSR, Slovakia; ARRS and MIZŠ, Slovenia; DSI/NRF, South Africa; MICINN, Spain; SRC and Wallenberg Foundation, Sweden; SERI, SNSF, and Cantons of Bern and Geneva, Switzerland; MOST, Taipei; TENMAK, Türkiye; STFC, United Kingdom; DOE and NSF, U.S. Individual groups and members have received support from BCKDF, CANARIE, CRC, and DRAC, Canada; PRIMUS 21/SCI/017 and UNCE SCI/013, Czech Republic; COST, ERC, ERDF, Horizon 2020, ICSC-NextGenerationEU, and Marie Skłodowska-Curie Actions, European Union; Investissements d’Avenir Labex, Investissements d’Avenir Idex, and ANR, France; DFG and AvH Foundation, Germany; Herakleitos, Thales, and Aristeia programs cofinanced by EU-ESF and the Greek NSRF, Greece; BSF-NSF and MINERVA, Israel; Norwegian Financial Mechanism 2014-2021, Norway; NCN and NAWA, Poland; La Caixa Banking Foundation, CERCA Programme Generalitat de Catalunya, and PROMETEO and GenT Programmes Generalitat Valenciana, Spain; Göran Gustafssons Stiftelse, Sweden; The Royal Society and Leverhulme Trust, United Kingdom. In addition, individual members wish to acknowledge support from CERN: European Organization for Nuclear Research (CERN PIAS); Chile: Agencia Nacional de Investigación y Desarrollo (FONDECYT 1190886, FONDECYT 1210400, FONDECYT 1230987); China: National Natural Science Foundation of China (NSFC—12175119, NSFC 12275265); European Union: European Research Council (ERC—948254, ERC 101089007), Horizon 2020 Framework Programme (MUCCA—CHIST-ERA-19-XAI-00), Italian Center for High Performance Computing, Big Data and Quantum

Computing (ICSC, NextGenerationEU); France: Agence Nationale de la Recherche (ANR-20-CE31-0013, ANR-21-CE31-0022), Investissements d’Avenir Labex (ANR-11-LABX-0012); Germany: Baden-Württemberg Stiftung (BW Stiftung-Postdoc Eliteprogramme), Deutsche Forschungsgemeinschaft (DFG—469666862, DFG—CR 312/5-2); Italy: Istituto Nazionale di Fisica Nucleare (ICSC, NextGenerationEU); Japan: Japan Society for the Promotion of Science (JSPS KAKENHI 22H01227, JSPS KAKENHI 22KK0227, JSPS KAKENHI JP21H05085, JSPS KAKENHI JP22H04944); Netherlands: Netherlands Organisation for Scientific Research (NWO Veni 2020—VI.Veni.202.179); Norway: Research Council of Norway (RCN-314472); Poland: Polish National Agency for Academic Exchange (PPN/PPO/2020/1/00002/U/00001), Polish National Science Centre (NCN 2021/42/E/ST2/00350, NCN OPUS nr 2022/47/B/ST2/03059, NCN UMO-2019/34/E/ST2/00393, UMO-2020/37/B/ST2/01043, UMO-2021/40/C/ST2/00187, UMO-2022/47/O/ST2/00148); Slovenia: Slovenian Research Agency (ARIS Grant No. J1-3010); Spain: BBVA Foundation (LEO22-1-603), Generalitat Valenciana (Artemisa, FEDER, IDIFEDER/2018/048), Ministry of Science and Innovation (RYC2019-028510-I, RYC2020-030254-I), PROMETEO and GenT Programmes Generalitat Valenciana (CIDEAGENT/2019/023, CIDEAGENT/2019/027); Sweden: Swedish Research Council (VR 2022-03845), Knut and Alice Wallenberg Foundation (KAW 2017.0100, KAW 2018.0157, KAW 2019.0447, KAW 2022.0358); Switzerland: Swiss National Science Foundation (SNSF—PCEFP2_194658); United Kingdom: Leverhulme Trust (Leverhulme Trust RPG-2020-004); U.S.: Neubauer Family Foundation.

Appendix A: Simulated data samples.—The signal samples are generated using the leading-order matrix elements with up to two extra partons using MadGraph [64] v2.9.5 and interfaced with PYTHIA8.306 [65] for simulating the subsequent decays, parton showering, and hadronization. The A14 tune [66] of PYTHIA is used with the NNPDF23lo PDF set. Matching between the matrix element and parton showering is performed following the CKKW-L prescription [67] with the merging scale set to 15 GeV. The signal MC samples were processed with a fast simulation [68], which relies on a parametrization of the calorimeter response [69].

The $W + \text{jet}$ and $Z + \text{jet}$ backgrounds are generated using SHERPAv2.2.11 [70] with the NNPDF30nnlo PDF set [71]. The diboson sample is generated with SHERPAv2.2.2. The $t\bar{t}$ and single top-quark processes are generated at NLO with Powheg-Box [72–75] v2 and interfaced with PYTHIA8.230 with the A14 tune. The diagram removal scheme [76] is employed in the simulation of single top-quark production to account for interference between the $t\bar{t}$ and Wt processes. The NNPDF30nnlo PDFs are used for all the MC samples of the SM processes.

Appendix B: Validation of background estimation.— This appendix describes the event selections used to validate the background estimates introduced in the main text. See Supplemental Material [53] associated with this Letter for schematics to illustrate the region layout as well as tables summarizing the selection criteria.

τ track background: In the following, regions with a symbol τ_h or τ_ℓ (referred to as τ_h regions or τ_ℓ regions) are dominated by the hadronic and leptonic τ decays, respectively. The τ_h (τ_ℓ) regions are defined by requiring no (one) lepton in the event. In the τ_ℓ regions, the electron (muon) is required to fail either of the following requirements; the tight identification criteria [37], transverse impact parameter selection $|d_0|/\sigma(d_0) < 3$, or the “Loose_VarRad” isolation criteria [77] (transverse impact parameter selection $|d_0|/\sigma(d_0) < 5$, $|\eta| < 2.5$, or the “PflowLoose” isolation criteria [38]). This requirement enhances the contribution of leptons from τ decays with respect to the ordinary prompt leptons. The p_T^{recoil} variable serves as a proxy for the p_T of the W boson and refers to $E_T^{\text{miss}} [|\mathbf{p}_T(\ell) + \mathbf{p}_T^{\text{miss}}|]$ in regions with no (one) lepton.

The $W(\rightarrow \tau\nu) + \text{jet}$ MC sample is normalized to the data in CR- τ_h and CR- τ_ℓ to obtain the estimate in the SR. These CRs are defined by a higher track p_T requirement (8–20 GeV) where the τ track background dominates with $>90\%$ purity. The $S(d_0)$ selection is loosened to acquire larger data statistics. The extrapolation over the track p_T is validated in VR- τ_h and VR- τ_ℓ , where the intermediate track p_T range (5–8 GeV) is selected. To avoid signal contamination in the VRs, the E_T^{miss} selection is shifted to $300 < E_T^{\text{miss}} < 400$ GeV. To validate the track p_T extrapolation in an isolated way, the estimates in the VRs are obtained by normalizing the MC in CRs with the same shifted E_T^{miss} requirement. These CRs are denoted CR2- τ_h and CR2- τ_ℓ . The schematic of the region segmentation is shown in Supplemental Material [53].

QCD track background: Control region CR-1 μ , dominated by $W(\rightarrow \mu\nu) + \text{jets}$, is used to extract the shape of the $S(d_0)$ distribution. This is normalized to each CR [$S(d_0) < 8$] to get the estimate in the adjacent SR or VR [$S(d_0) > 8$]. Validation regions VR-1 e , VR-2 ℓ , and VR-1 γ are defined with one electron, two leptons, and one photon, respectively, where the corresponding dominant contributions are from $W(\rightarrow e\nu) + \text{jet}$, $Z(\rightarrow \ell\ell) + \text{jet}$, and $\gamma + \text{jet}$ production. The choice of the VRs is motivated by their similar matrix element to that of the $Z(\rightarrow \nu\nu) + \text{jets}$, the main physics process yielding the QCD track background in the SR. The purities of $W/Z/\gamma + \text{jets}$ are $>90\%$ except for VR(CR)-1 γ , which has a $\sim 30\%$ contribution from QCD multijet production. However, the shape of the $S(d_0)$ distribution from these multijet events is found to be nearly identical to that of $\gamma + \text{jets}$ production. The QCD track background considered in this fully data-driven estimate is therefore defined by events with the production of $W(\rightarrow \mu\nu) + \text{jets}$ in VR(CR)-1 μ ; $W(\rightarrow e\nu) + \text{jets}$ in

VR(CR)-1 e ; $Z(\rightarrow \ell\ell) + \text{jets}$ in VR(CR)-2 ℓ ; $\gamma + \text{jets}$ and multijet in VR(CR)-1 γ . The contribution from other backgrounds is modeled by the MC simulation in each VR and the associated CR, which is subtracted from the data in the $S(d_0)$ shape extraction or the normalization in the CRs. The schematic of the region’s segmentation is shown in Supplemental Material [53].

The single-electron (single-photon) trigger is used to collect events with electrons (photons), and the E_T^{miss} trigger is used to record events with large E_T^{miss} or muons. Muons are counted as missing objects at the E_T^{miss} trigger. Additional quality requirements are applied for electrons, muons, and photons for regions requiring those; the tight identification criteria [37], transverse impact parameter selection $|d_0|/\sigma(d_0) < 3$, and Loose_VarRad isolation criteria [77] are required for the electrons; transverse impact parameter selection $|d_0|/\sigma(d_0) < 5$, $|\eta| < 2.5$ and the PflowLoose isolation [38] are imposed for the muons; the tight isolation criteria [37] and $p_T > 200$ GeV are applied for the photons. These are to suppress the fake lepton and photon contributions from hadronic jets or the nonprompt leptons from bottom and charm hadron decays. Variable p_T^{recoil} is defined as the proxy for the p_T of the $W/Z/\gamma$ boson, i.e., $|\mathbf{p}_T(\ell) + \mathbf{p}_T^{\text{miss}}|$ in CR-1 μ and VR(CR)-1 e ; $|\mathbf{p}_T(\ell_1) + \mathbf{p}_T(\ell_2) + \mathbf{p}_T^{\text{miss}}|$ in VR(CR)-2 ℓ ; $|\mathbf{p}_T(\gamma) + \mathbf{p}_T^{\text{miss}}|$ in VR(CR)-1 γ ; and E_T^{miss} in other regions. The kinematic selection of the VRs is aligned as much as possible to the SR to ensure the same phase space is probed,

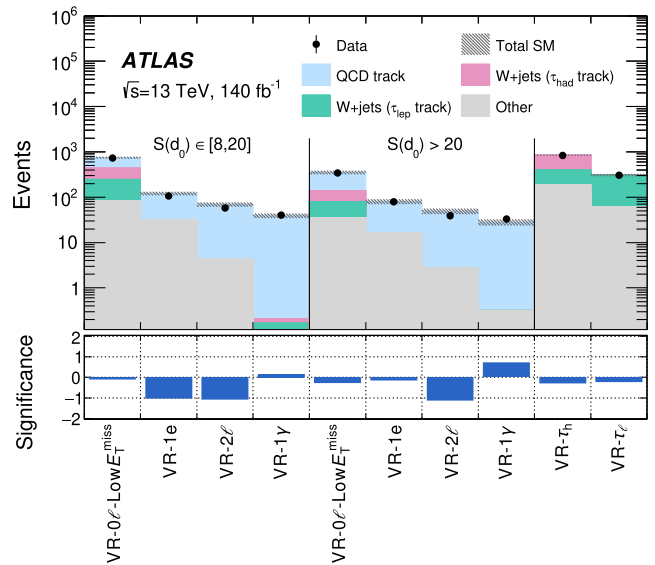


FIG. 4. Comparisons of the observed data and the expected SM background in the VRs after the profile likelihood fit in the CRs. The hatched band indicates the total uncertainty on the SM background expectation, including both statistical and systematic uncertainties. The bottom panel shows the statistical significances [78] of the discrepancy between the expected and the observed event yields.

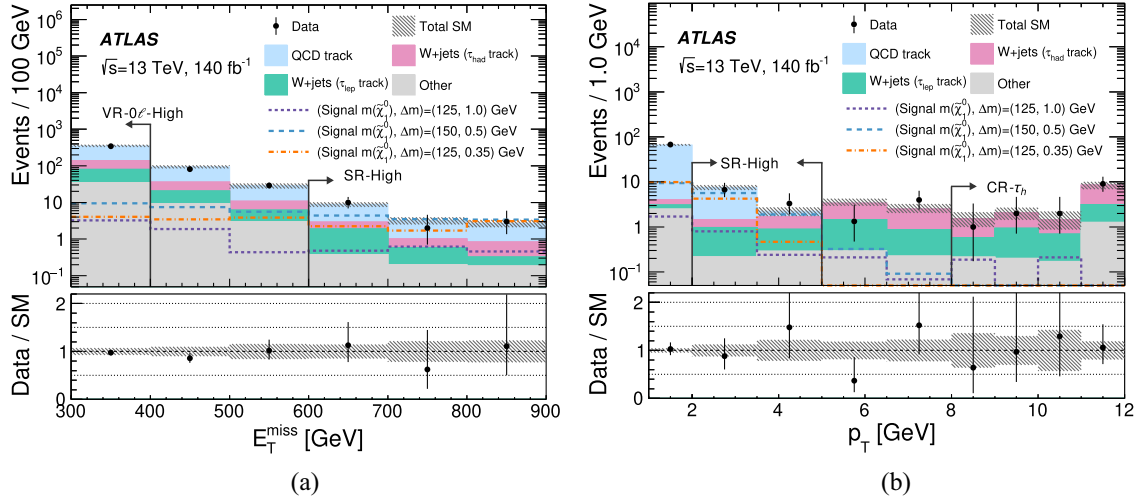


FIG. 5. Distributions of E_T^{miss} and track p_T in, and near, the phase-space of SR-high. The selection criterion on the variable shown by each plot is removed, while the arrow indicates the cut value to define the region. The SM background expectation is shown as a histogram stack, and a few representative signal models are overlaid. The last bin includes the overflow. The hatched band indicates the uncertainty on the mean value of the SM background expectation, while the error bars on the black dots represent the Poisson error associated with the event yields.

while a minimal set of additional selections are introduced to enhance the purity of $W/Z/\gamma + \text{jet}$ events in respective regions.

Hybrid validation region: Validation region VR-0 ℓ -low E_T^{miss} is designed to validate the modeling of both the τ track and QCD track backgrounds, for which the contributions are nearly equal. This VR is defined by shifting the E_T^{miss} selection to $300 < E_T^{\text{miss}} < 400$ GeV with respect to the SR ($E_T^{\text{miss}} > 600$ GeV). The τ track background is estimated by normalizing the MC in the low E_T^{miss} control regions (CR2- τ_h and CR2- τ_ℓ), and the QCD track background is derived from the $S(d_0)$ shape that is simultaneously normalized in CR-0 ℓ -low E_T^{miss} .

Fit results: Each VR is estimated by a separate profile likelihood fit, except for the τ track VRs where the estimates of VR- τ_h and VR- τ_ℓ are obtained from a single fit. The associated CR(s) are used to constrain the likelihood, including all the systematic uncertainties described in the main text, as well as the uncertainties on the lepton and photon isolation efficiencies. Any potential signal contamination is expected to be below 5% in all of the CRs and VRs and is therefore ignored in the fits. The data and background estimates in the VRs are summarized in Fig. 4, where they are shown to be consistent within the uncertainty.

Appendix C: Postfit kinematic distributions in SR-high.—This appendix shows additional postfit distributions of kinematic variables important to the analysis. Figure 5 shows the E_T^{miss} and track p_T distributions in, and near, the phase space of SR-High.

- [1] Y. Golfand and E. Likhtman, Extension of the algebra of Poincare group generators and violation of P invariance, Pis'ma Zh. Eksp. Teor. Fiz. **13**, 452 (1971) [*JETP Lett.* **13**, 323 (1971)].
- [2] D. Volkov and V. Akulov, Is the neutrino a goldstone particle?, *Phys. Lett.* **46B**, 109 (1973).
- [3] J. Wess and B. Zumino, Supergauge transformations in four dimensions, *Nucl. Phys.* **B70**, 39 (1974).
- [4] J. Wess and B. Zumino, Supergauge invariant extension of quantum electrodynamics, *Nucl. Phys.* **B78**, 1 (1974).
- [5] S. Ferrara and B. Zumino, Supergauge invariant Yang-Mills theories, *Nucl. Phys.* **B79**, 413 (1974).
- [6] A. Salam and J. Strathdee, Super-symmetry and non-Abelian gauges, *Phys. Lett.* **51B**, 353 (1974).
- [7] R. Barbieri and G. Giudice, Upper bounds on supersymmetric particle masses, *Nucl. Phys.* **B306**, 63 (1988).
- [8] B. de Carlos and J. Casas, One-loop analysis of the electroweak breaking in supersymmetric models and the fine-tuning problem, *Phys. Lett. B* **309**, 320 (1993).
- [9] P. Fayet, Supersymmetry and weak, electromagnetic and strong interactions, *Phys. Lett.* **64B**, 159 (1976).
- [10] P. Fayet, Spontaneously broken supersymmetric theories of weak, electromagnetic and strong interactions, *Phys. Lett.* **69B**, 489 (1977).
- [11] G. R. Farrar and P. Fayet, Phenomenology of the production, decay, and detection of new hadronic states associated with supersymmetry, *Phys. Lett.* **76B**, 575 (1978).
- [12] M. Cirelli, A. Strumia, and M. Tamburini, Cosmology and astrophysics of minimal dark matter, *Nucl. Phys.* **B787**, 152 (2007).
- [13] K. Kowalska and E. M. Sessolo, The discreet charm of Higgsino dark matter: A pocket review, *Adv. High Energy Phys.* **2018**, 1 (2018).

- [14] N. Nagata and S. Shirai, Higgsino dark matter in high-scale supersymmetry, *J. High Energy Phys.* **01** (2015) 029.
- [15] ATLAS Collaboration, Search for long-lived charginos based on a disappearing-track signature in pp collisions at $\sqrt{s} = 13$ TeV with the ATLAS detector, *J. High Energy Phys.* **06** (2018) 022.
- [16] ATLAS Collaboration, Search for long-lived charginos based on a disappearing-track signature using 136 fb^{-1} of pp collisions at $\sqrt{s} = 13$ TeV with the ATLAS detector, *Eur. Phys. J. C* **82**, 606 (2022).
- [17] CMS Collaboration, Search for disappearing tracks as a signature of new long-lived particles in proton-proton collisions at $\sqrt{s} = 13$ TeV, *J. High Energy Phys.* **08** (2018) 016.
- [18] CMS Collaboration, Search for disappearing tracks in proton-proton collisions at $\sqrt{s} = 13$ TeV, *Phys. Lett. B* **806**, 135502 (2020).
- [19] ATLAS Collaboration, Searches for electroweak production of supersymmetric particles with compressed mass spectra in $\sqrt{s} = 13$ TeV pp collisions with the ATLAS detector, *Phys. Rev. D* **101**, 052005 (2020).
- [20] ATLAS Collaboration, Search for chargino-neutralino pair production in final states with three leptons and missing transverse momentum in $\sqrt{s} = 13$ TeV pp collisions with the ATLAS detector, *Eur. Phys. J. C* **81**, 1118 (2021).
- [21] CMS Collaboration, Search for electroweak production of charginos and neutralinos in proton-proton collisions at $\sqrt{s} = 13$ TeV, *J. High Energy Phys.* **04** (2022) 147.
- [22] ALEPH, DELPHI, L3, OPAL Experiments Collaborations, Combined LEP chargino results, up to 208 GeV for low DM, Report No. LEPSUSYWG/02-04.1, 2002, http://lepsusy.web.cern.ch/lepsusy/www/inoslowdmsummer02/charginolowdm_pub.html.
- [23] H. Fukuda, N. Nagata, H. Oide, H. Otono, and S. Shirai, Cornering Higgsinos using soft displaced tracks, *Phys. Rev. Lett.* **124**, 101801 (2020).
- [24] ATLAS uses a right-handed coordinate system with its origin at the nominal interaction point (IP) in the center of the detector and the z axis along the beam pipe. The x axis points from the IP to the center of the LHC ring, and the y axis points upward. Cylindrical coordinates (r, ϕ) are used in the transverse plane, ϕ being the azimuthal angle around the z axis. The pseudorapidity is defined in terms of the polar angle θ as $\eta = -\ln \tan(\theta/2)$. Angular distance is measured in units of $\Delta R \equiv \sqrt{(\Delta\eta)^2 + \Delta\phi^2}$.
- [25] ATLAS Collaboration, The ATLAS experiment at the CERN Large Hadron Collider, *J. Instrum.* **3**, S08003 (2008).
- [26] ATLAS Collaboration, Search for new phenomena in events with an energetic jet and missing transverse momentum in pp collisions at $\sqrt{s} = 13$ TeV with the ATLAS detector, *Phys. Rev. D* **103**, 112006 (2021).
- [27] CMS Collaboration, Search for new particles in events with energetic jets and large missing transverse momentum in proton-proton collisions at $\sqrt{s} = 13$ TeV, *J. High Energy Phys.* **11** (2021) 153.
- [28] R. Pasechnik, V.A. Beylin, V.I. Kuksa, and G.M. Vereshkov, Neutralino-nucleon interaction in the split SUSY scenario of the dark matter, *Int. J. Mod. Phys. A* **24**, 6051 (2009).
- [29] ATLAS Collaboration, Impact parameter resolutions in di-jet events, Report No. ATL-IDTR-2018-008, 2018, <https://atlas.web.cern.ch/Atlas/GROUPS/PHYSICS/PLOTS/IDTR-2018-008/>.
- [30] ATLAS Collaboration, Performance of the missing transverse momentum triggers for the ATLAS detector during run-2 data taking, *J. High Energy Phys.* **08** (2020) 080.
- [31] ATLAS Collaboration, Performance of electron and photon triggers in ATLAS during LHC run 2, *Eur. Phys. J. C* **80**, 47 (2020).
- [32] ATLAS Collaboration, The ATLAS Collaboration software and firmware, Report No. ATL-SOFT-PUB-2021-001, 2021, <https://cds.cern.ch/record/2767187>.
- [33] ATLAS Collaboration, Jet reconstruction and performance using particle flow with the ATLAS detector, *Eur. Phys. J. C* **77**, 466 (2017).
- [34] M. Cacciari, G. P. Salam, and G. Soyez, The anti- k_t jet clustering algorithm, *J. High Energy Phys.* **04** (2008) 063.
- [35] M. Cacciari, G. P. Salam, and G. Soyez, FastJet user manual, *Eur. Phys. J. C* **72**, 1896 (2012).
- [36] ATLAS Collaboration, Performance of pileup mitigation techniques for jets in pp collisions at $\sqrt{s} = 8$ TeV using the ATLAS detector, *Eur. Phys. J. C* **76**, 581 (2016).
- [37] ATLAS Collaboration, Electron and photon performance measurements with the ATLAS detector using the 2015–2017 LHC proton-proton collision data, *J. Instrum.* **14**, P12006 (2019).
- [38] ATLAS Collaboration, Muon reconstruction and identification efficiency in ATLAS using the full run 2 pp collision data set at $\sqrt{s} = 13$ TeV, *Eur. Phys. J. C* **81**, 578 (2021).
- [39] ATLAS Collaboration, Search for charginos and neutralinos in final states with two boosted hadronically decaying bosons and missing transverse momentum in pp collisions at $\sqrt{s} = 13$ TeV with the ATLAS detector, *Phys. Rev. D* **104**, 112010 (2021).
- [40] ATLAS Collaboration, Performance of missing transverse momentum reconstruction with the ATLAS detector using proton-proton collisions at $\sqrt{s} = 13$ TeV, *Eur. Phys. J. C* **78**, 903 (2018).
- [41] ATLAS Collaboration, Early inner detector tracking performance in the 2015 data at $\sqrt{s} = 13$ TeV, Report No. ATL-PHYS-PUB-2015-051, 2015, <https://cds.cern.ch/record/2110140>.
- [42] ATLAS Collaboration, K_S^0 and Λ production in pp interactions at $\sqrt{s} = 0.9$ and 7 TeV measured with the ATLAS detector at the LHC, *Phys. Rev. D* **85**, 012001 (2012).
- [43] ATLAS Collaboration, Performance of the reconstruction of large impact parameter tracks in the inner detector of ATLAS, *Eur. Phys. J. C* **83**, 1081 (2023).
- [44] W. Beenakker, M. Klasen, M. Krämer, T. Plehn, M. Spira, and P. M. Zerwas, Production of charginos, neutralinos, and sleptons at hadron colliders, *Phys. Rev. Lett.* **83**, 3780 (1999); **100**, 029901(E) (2008).
- [45] J. Debove, B. Fuks, and M. Klasen, Threshold resummation for gaugino pair production at hadron colliders, *Nucl. Phys.* **B842**, 51 (2011).
- [46] B. Fuks, M. Klasen, D.R. Lamprea, and M. Rothering, Gaugino production in proton-proton collisions at a center-of-mass energy of 8 TeV, *J. High Energy Phys.* **10** (2012) 081.

- [47] B. Fuks, M. Klasen, D. R. Lamprea, and M. Rothering, Precision predictions for electroweak superpartner production at hadron colliders with RESUMMINO, *Eur. Phys. J. C* **73**, 2480 (2013).
- [48] J. Fiaschi and M. Klasen, Neutralino-chargino pair production at NLO + NLL with resummation-improved parton density functions for LHC run II, *Phys. Rev. D* **98**, 055014 (2018).
- [49] C. Borschensky, M. Krämer, A. Kulesza, M. Mangano, S. Padhi, T. Plehn, and X. Portell, Squark and gluino production cross sections in pp collisions at $\sqrt{s} = 13, 14, 33$ and 100 TeV, *Eur. Phys. J. C* **74**, 3174 (2014).
- [50] J. Butterworth *et al.*, PDF4LHC recommendations for LHC run II, *J. Phys. G* **43**, 023001 (2016).
- [51] ATLAS Collaboration, Characterisation and mitigation of beam-induced backgrounds observed in the ATLAS detector during the 2011 proton-proton run, *J. Instrum.* **8**, P07004 (2013).
- [52] ATLAS Collaboration, Selection of jets produced in 13 TeV proton-proton collisions with the ATLAS detector, Report No. ATLAS-CONF-2015-029, 2015, <https://cds.cern.ch/record/2037702>.
- [53] See Supplemental Material at <http://link.aps.org/supplemental/10.1103/PhysRevLett.132.221801> for schematic illustrations of the region layout and tables summarizing the selection criteria.
- [54] G. Cowan, K. Cranmer, E. Gross, and O. Vitells, Asymptotic formulae for likelihood-based tests of new physics, *Eur. Phys. J. C* **71**, 1554 (2011); **73**, 2501(E) (2013).
- [55] ATLAS Collaboration, Electron reconstruction and identification in the ATLAS experiment using the 2015 and 2016 LHC proton-proton collision data at $\sqrt{s} = 13$ TeV, *Eur. Phys. J. C* **79**, 639 (2019).
- [56] ATLAS Collaboration, Electron and photon energy calibration with the ATLAS detector using 2015–2016 LHC proton-proton collision data, *J. Instrum.* **14**, P03017 (2019).
- [57] ATLAS Collaboration, Jet energy scale and resolution measured in proton-proton collisions at $\sqrt{s} = 13$ TeV with the ATLAS detector, *Eur. Phys. J. C* **81**, 689 (2021).
- [58] ATLAS Collaboration, Tagging and suppression of pileup jets with the ATLAS detector, Report No. ATLASCONF-2014-018, 2014, <https://cds.cern.ch/record/1700870>.
- [59] G. Avoni *et al.*, The new LUCID-2 detector for luminosity measurement and monitoring in ATLAS, *J. Instrum.* **13**, P07017 (2018).
- [60] ATLAS Collaboration, Multi-boson simulation for 13 TeV ATLAS analyses, Report No. ATL-PHYS-PUB-2016-002, 2016, <https://cds.cern.ch/record/2119986>.
- [61] A. L. Read, Presentation of search results: the CL_s technique, *J. Phys. G* **28**, 2693 (2002).
- [62] S. Thomas and J. D. Wells, Phenomenology of massive vectorlike doublet leptons, *Phys. Rev. Lett.* **81**, 34 (1998).
- [63] ATLAS Collaboration, ATLAS computing acknowledgements, Report No. ATL-SOFT-PUB-2023-001, 2023, <https://cds.cern.ch/record/2869272>.
- [64] J. Alwall, R. Frederix, S. Frixione, V. Hirschi, F. Maltoni, O. Mattelaer, H.-S. Shao, T. Stelzer, P. Torrielli, and M. Zaro, The automated computation of tree-level and next-to-leading order differential cross sections, and their matching to parton shower simulations, *J. High Energy Phys.* **07** (2014) 079.
- [65] T. Sjöstrand, S. Ask, J. R. Christiansen, R. Corke, N. Desai, P. Ilten, S. Mrenna, S. Prestel, C. O. Rasmussen, and P. Z. Skands, An introduction to PYTHIA8.2, *Comput. Phys. Commun.* **191**, 159 (2015).
- [66] ATLAS Collaboration, ATLAS PYTHIA8 tunes to 7 TeV data, Report No. ATL-PHYS-PUB-2014-021, 2014, <https://cds.cern.ch/record/1966419>.
- [67] L. Lönnblad and S. Prestel, Matching tree-level matrix elements with interleaved showers, *J. High Energy Phys.* **03** (2012) 019.
- [68] ATLAS Collaboration, The ATLAS simulation infrastructure, *Eur. Phys. J. C* **70**, 823 (2010).
- [69] ATLAS Collaboration, The simulation principle and performance of the ATLAS fast calorimeter simulation FastCaloSim, Report No. ATL-PHYS-PUB-2010-013, 2010, <https://cds.cern.ch/record/1300517>.
- [70] E. Bothmann *et al.*, Event generation with SHERPA2.2, *SciPost Phys.* **7**, 034 (2019).
- [71] R. D. Ball *et al.* (NNPDF Collaboration), Parton distributions for the LHC run II, *J. High Energy Phys.* **04** (2015) 040.
- [72] S. Frixione, G. Ridolfi, and P. Nason, A positive-weight next-to-leading-order Monte Carlo for heavy flavour hadroproduction, *J. High Energy Phys.* **09** (2007) 126.
- [73] P. Nason, A new method for combining NLO QCD with shower Monte Carlo algorithms, *J. High Energy Phys.* **11** (2004) 040.
- [74] S. Frixione, P. Nason, and C. Oleari, Matching NLO QCD computations with parton shower simulations: The POWHEG method, *J. High Energy Phys.* **11** (2007) 070.
- [75] S. Alioli, P. Nason, C. Oleari, and E. Re, A general framework for implementing NLO calculations in shower Monte Carlo programs: The POWHEG BOX, *J. High Energy Phys.* **06** (2010) 043.
- [76] S. Frixione, E. Laenen, P. Motylinski, C. White, and B. R. Webber, Single-top hadroproduction in association with a W boson, *J. High Energy Phys.* **07** (2008) 029.
- [77] ATLAS Collaboration, Electron and photon efficiencies in LHC run 2 with the ATLAS experiment, [arXiv:2308.13362](https://arxiv.org/abs/2308.13362).
- [78] R. D. Cousins, J. T. Linnemann, and J. Tucker, Evaluation of three methods for calculating statistical significance when incorporating a systematic uncertainty into a test of the background-only hypothesis for a Poisson process, *Nucl. Instrum. Methods Phys. Res., Sect. A* **595**, 480 (2008).

G. Aad¹⁰³, E. Aakvaag¹⁶, B. Abbott¹²¹, K. Abeling⁵⁵, N. J. Abicht⁴⁹, S. H. Abidi²⁹, M. Aboelela⁴⁴, A. Aboulhorma^{35e}, H. Abramowicz¹⁵², H. Abreu¹⁵¹, Y. Abulaiti¹¹⁸, B. S. Acharya^{69a,69b,b}, A. Ackermann^{63a}

- C. Adam Bourdarios⁴, L. Adamczyk^{86a}, S. V. Addepalli²⁶, M. J. Addison¹⁰², J. Adelman¹¹⁶, A. Adiguzel^{21c}, T. Adye¹³⁵, A. A. Affolder¹³⁷, Y. Afik³⁹, M. N. Agaras¹³, J. Agarwala^{73a,73b}, A. Aggarwal¹⁰¹, C. Agheorghiesei^{27c}, A. Ahmad³⁶, F. Ahmadov^{38,c}, W. S. Ahmed¹⁰⁵, S. Ahuja⁹⁶, X. Ai^{62e}, G. Aielli^{76a,76b}, A. Aikot¹⁶⁴, M. Ait Tamliah^{35e}, B. Aitbenchikh^{35a}, I. Aizenberg¹⁷⁰, M. Akbiyik¹⁰¹, T. P. A. Åkesson⁹⁹, A. V. Akimov³⁷, D. Akiyama¹⁶⁹, N. N. Akolkar²⁴, S. Aktas^{21a}, K. Al Khoury⁴¹, G. L. Alberghi^{23b}, J. Albert¹⁶⁶, P. Albicocco⁵³, G. L. Albouy⁶⁰, S. Alderweireldt⁵², Z. L. Alegria¹²², M. Aleksa³⁶, I. N. Aleksandrov³⁸, C. Alexa^{27b}, T. Alexopoulos¹⁰, F. Alfonsi^{23b}, M. Algren⁵⁶, M. Alhroob¹⁴², B. Ali¹³³, H. M. J. Ali⁹², S. Ali¹⁴⁹, S. W. Alibocus⁹³, M. Aliev^{33c}, G. Alimonti^{71a}, W. Alkakhki⁵⁵, C. Allaire⁶⁶, B. M. M. Allbrooke¹⁴⁷, J. F. Allen⁵², C. A. Allendes Flores^{138f}, P. P. Allport²⁰, A. Aloisio^{72a,72b}, F. Alonso⁹¹, C. Alpigiani¹³⁹, M. Alvarez Estevez¹⁰⁰, A. Alvarez Fernandez¹⁰¹, M. Alves Cardoso⁵⁶, M. G. Alviggi^{72a,72b}, M. Aly¹⁰², Y. Amaral Coutinho^{83b}, A. Ambler¹⁰⁵, C. Amelung³⁶, M. Amerl¹⁰², C. G. Ames¹¹⁰, D. Amidei¹⁰⁷, K. J. Amirie¹⁵⁶, S. P. Amor Dos Santos^{131a}, K. R. Amos¹⁶⁴, S. An⁸⁴, V. Ananiev¹²⁶, C. Anastopoulos¹⁴⁰, T. Andeen¹¹, J. K. Anders³⁶, S. Y. Andrean^{47a,47b}, A. Andreatza^{71a,71b}, S. Angelidakis⁹, A. Angerami^{41,d}, A. V. Anisenkov³⁷, A. Annovi^{74a}, C. Antel⁵⁶, M. T. Anthony¹⁴⁰, E. Antipov¹⁴⁶, M. Antonelli⁵³, F. Anulli^{75a}, M. Aoki⁸⁴, T. Aoki¹⁵⁴, J. A. Aparisi Pozo¹⁶⁴, M. A. Aparo¹⁴⁷, L. Aperio Bella⁴⁸, C. Appelt¹⁸, A. Apyan²⁶, S. J. Arbiol Val⁸⁷, C. Arcangeletti⁵³, A. T. H. Arce⁵¹, E. Arena⁹³, J-F. Arguin¹⁰⁹, S. Argyropoulos⁵⁴, J.-H. Arling⁴⁸, O. Arnaez⁴, H. Arnold¹¹⁵, G. Artoni^{75a,75b}, H. Asada¹¹², K. Asai¹¹⁹, S. Asai¹⁵⁴, N. A. Asbah³⁶, K. Assamagan²⁹, R. Astalos^{28a}, K. S. V. Astrand⁹⁹, S. Atashi¹⁶⁰, R. J. Atkin^{33a}, M. Atkinson¹⁶³, H. Atmani^{35f}, P. A. Atmasiddha¹²⁹, K. Augsten¹³³, S. Auricchio^{72a,72b}, A. D. Auriol²⁰, V. A. Austrup¹⁰², G. Avolio³⁶, K. Axiotis⁵⁶, G. Azuelos^{109,e}, D. Babal^{28b}, H. Bachacou¹³⁶, K. Bachas^{153,f}, A. Bachi³⁴, F. Backman^{47a,47b}, A. Badea³⁹, T. M. Baer¹⁰⁷, P. Bagnaia^{75a,75b}, M. Bahmani¹⁸, D. Bahner⁵⁴, K. Bai¹²⁴, A. J. Bailey¹⁶⁴, J. T. Baines¹³⁵, L. Baines⁹⁵, O. K. Baker¹⁷³, E. Bakos¹⁵, D. Bakshi Gupta⁸, V. Balakrishnan¹²¹, R. Balasubramanian¹¹⁵, E. M. Baldin³⁷, P. Balek^{86a}, E. Ballabene^{23b,23a}, F. Balli¹³⁶, L. M. Baltes^{63a}, W. K. Balunas³², J. Balz¹⁰¹, E. Banas⁸⁷, M. Bandieramonte¹³⁰, A. Bandyopadhyay²⁴, S. Bansal²⁴, L. Barak¹⁵², M. Barakat⁴⁸, E. L. Barberio¹⁰⁶, D. Barberis^{57b,57a}, M. Barbero¹⁰³, M. Z. Barel¹¹⁵, K. N. Barends^{33a}, T. Barillari¹¹¹, M-S. Barisits³⁶, T. Barklow¹⁴⁴, P. Baron¹²³, D. A. Baron Moreno¹⁰², A. Baroncelli^{62a}, G. Barone²⁹, A. J. Barr¹²⁷, J. D. Barr⁹⁷, F. Barreiro¹⁰⁰, J. Barreiro Guimarães da Costa^{14a}, U. Barron¹⁵², M. G. Barros Teixeira^{131a}, S. Barsov³⁷, F. Bartels^{63a}, R. Bartoldus¹⁴⁴, A. E. Barton⁹², P. Bartos^{28a}, A. Basan¹⁰¹, M. Baselga⁴⁹, A. Bassalat^{66,g}, M. J. Basso^{157a}, R. L. Bates⁵⁹, S. Batlamous^{35e}, B. Batool¹⁴², M. Battaglia¹³⁷, D. Battulga¹⁸, M. Bauce^{75a,75b}, M. Bauer³⁶, P. Bauer²⁴, L. T. Bazzano Hurrell³⁰, J. B. Beacham⁵¹, T. Beau¹²⁸, J. Y. Beaucamp⁹¹, P. H. Beauchemin¹⁵⁹, P. Bechtel²⁴, H. P. Beck^{19,h}, K. Becker¹⁶⁸, A. J. Beddall⁸², V. A. Bednyakov³⁸, C. P. Bee¹⁴⁶, L. J. Beemster¹⁵, T. A. Beermann³⁶, M. Begalli^{83d}, M. Begel²⁹, A. Behera¹⁴⁶, J. K. Behr⁴⁸, J. F. Beirer³⁶, F. Beisiegel²⁴, M. Belfkir^{117b}, G. Bella¹⁵², L. Bellagamba^{23b}, A. Bellerive³⁴, P. Bellos²⁰, K. Beloborodov³⁷, D. Benckekroun^{35a}, F. Bendebba^{35a}, Y. Benhammou¹⁵², K. C. Benkendorfer⁶¹, L. Beresford⁴⁸, M. Beretta⁵³, E. Bergeas Kuutmann¹⁶², N. Berger⁴, B. Bergmann¹³³, J. Beringer^{17a}, G. Bernardi⁵, C. Bernius¹⁴⁴, F. U. Bernlochner²⁴, F. Bernon^{36,103}, A. Berrocal Guardia¹³, T. Berry⁹⁶, P. Berta¹³⁴, A. Berthold⁵⁰, S. Bethke¹¹¹, A. Betti^{75a,75b}, A. J. Bevan⁹⁵, N. K. Bhalla⁵⁴, M. Bhamjee^{33c}, S. Bhatta¹⁴⁶, D. S. Bhattacharya¹⁶⁷, P. Bhattarai¹⁴⁴, K. D. Bhide⁵⁴, V. S. Bhopatkar¹²², R. M. Bianchi¹³⁰, G. Bianco^{23b,23a}, O. Biebel¹¹⁰, R. Bielski¹²⁴, M. Biglietti^{77a}, C. S. Billingsley⁴⁴, M. Bindi⁵⁵, A. Bingul^{21b}, C. Bini^{75a,75b}, A. Biondini⁹³, C. J. Birch-sykes¹⁰², G. A. Bird³², M. Birman¹⁷⁰, M. Biros¹³⁴, S. Biryukov¹⁴⁷, T. Bisanz⁴⁹, E. Bisceglie^{43b,43a}, J. P. Biswal¹³⁵, D. Biswas¹⁴², K. Bjørke¹²⁶, I. Bloch⁴⁸, A. Blue⁵⁹, U. Blumenschein⁹⁵, J. Blumenthal¹⁰¹, V. S. Bobrovnikov³⁷, M. Boehler⁵⁴, B. Boehm¹⁶⁷, D. Bogavac³⁶, A. G. Bogdanchikov³⁷, C. Bohm^{47a}, V. Boisvert⁹⁶, P. Bokan³⁶, T. Bold^{86a}, M. Bomben⁵, M. Bona⁹⁵, M. Boonekamp¹³⁶, C. D. Booth⁹⁶, A. G. Borbély⁵⁹, I. S. Bordulev³⁷, H. M. Borecka-Bielska¹⁰⁹, G. Borissov⁹², D. Bortoletto¹²⁷, D. Boscherini^{23b}, M. Bosman¹³, J. D. Bossio Sola³⁶, K. Bouaouda^{35a}, N. Bouchhar¹⁶⁴, J. Boudreau¹³⁰, E. V. Bouhova-Thacker⁹², D. Boumediene⁴⁰, R. Bouquet^{57b,57a}, A. Boveia¹²⁰, J. Boyd³⁶, D. Boye²⁹, I. R. Boyko³⁸, J. Bracinik²⁰, N. Brahimi⁴, G. Brandt¹⁷², O. Brandt³², F. Braren⁴⁸, B. Brau¹⁰⁴, J. E. Brau¹²⁴, R. Brenner¹⁷⁰, L. Brenner¹¹⁵, R. Brenner¹⁶², S. Bressler¹⁷⁰, D. Britton⁵⁹, D. Britzger¹¹¹, I. Brock²⁴, G. Brooijmans⁴¹, E. Brost²⁹, L. M. Brown¹⁶⁶, L. E. Bruce⁶¹, T. L. Bruckler¹²⁷, P. A. Bruckman de Renstrom⁸⁷

B. Brüers⁴⁸ A. Bruni^{23b} G. Bruni^{23b} M. Bruschi^{23b} N. Bruscano^{75a,75b} T. Buanes¹⁶ Q. Buat¹³⁹
 D. Buchin¹¹¹ A. G. Buckley⁵⁹ O. Bulekov³⁷ B. A. Bullard¹⁴⁴ S. Burdin⁹³ C. D. Burgard⁴⁹ A. M. Burger³⁶
 B. Burghgrave⁸ O. Burlayenko⁵⁴ J. T. P. Burr³² C. D. Burton¹¹ J. C. Burzynski¹⁴³ E. L. Busch⁴¹
 V. Büscher¹⁰¹ P. J. Bussey⁵⁹ J. M. Butler²⁵ C. M. Buttar⁵⁹ J. M. Butterworth⁹⁷ W. Buttinger¹³⁵
 C. J. Buxo Vazquez¹⁰⁸ A. R. Buzykaev³⁷ S. Cabrera Urbán¹⁶⁴ L. Cadamuro⁶⁶ D. Caforio⁵⁸ H. Cai¹³⁰
 Y. Cai^{14a,14e} Y. Cai^{14c} V. M. M. Cairo³⁶ O. Cakir^{3a} N. Calace³⁶ P. Calafiura^{17a} G. Calderini¹²⁸
 P. Calfayan⁶⁸ G. Callea⁵⁹ L. P. Caloba^{83b} D. Calvet⁴⁰ S. Calvet⁴⁰ M. Calvetti^{74a,74b} R. Camacho Toro¹²⁸
 S. Camarda³⁶ D. Camarero Munoz²⁶ P. Camarri^{76a,76b} M. T. Camerlingo^{72a,72b} D. Cameron³⁶ C. Camincher¹⁶⁶
 M. Campanelli⁹⁷ A. Camplani⁴² V. Canale^{72a,72b} A. C. Canbay^{3a} E. Canonero⁹⁶ J. Cantero¹⁶⁴ Y. Cao¹⁶³
 F. Capocasa²⁶ M. Capua^{43b,43a} A. Carbone^{71a,71b} R. Cardarelli^{76a} J. C. J. Cardenas⁸ F. Cardillo¹⁶⁴
 G. Carducci^{43b,43a} T. Carli³⁶ G. Carlino^{72a} J. I. Carlotta¹³ B. T. Carlson^{130,i} E. M. Carlson^{166,157a}
 L. Carminati^{71a,71b} A. Carnelli¹³⁶ M. Carnesale^{75a,75b} S. Caron¹¹⁴ E. Carquin^{138f} S. Carrá^{71a}
 G. Carratta^{23b,23a} A. M. Carroll¹²⁴ T. M. Carter⁵² M. P. Casado^{13,j} M. Caspar⁴⁸ F. L. Castillo⁴
 L. Castillo Garcia¹³ V. Castillo Gimenez¹⁶⁴ N. F. Castro^{131a,131e} A. Catinaccio³⁶ J. R. Catmore¹²⁶ T. Cavaliere⁴
 V. Cavaliere²⁹ N. Cavalli^{23b,23a} Y. C. Cekmecelioglu⁴⁸ E. Celebi^{21a} S. Cella³⁶ F. Celli¹²⁷
 M. S. Centonze^{70a,70b} V. Cepaitis⁵⁶ K. Cerny¹²³ A. S. Cerqueira^{83a} A. Cerri¹⁴⁷ L. Cerrito^{76a,76b} F. Cerutti^{17a}
 B. Cervato¹⁴² A. Cervelli^{23b} G. Cesarini⁵³ S. A. Cetin⁸² D. Chakraborty¹¹⁶ J. Chan^{17a} W. Y. Chan¹⁵⁴
 J. D. Chapman³² E. Chapon¹³⁶ B. Chargeishvili^{150b} D. G. Charlton²⁰ M. Chatterjee¹⁹ C. Chauhan¹³⁴
 Y. Che^{14c} S. Chekanov⁶ S. V. Chekulaev^{157a} G. A. Chelkov^{38,k} A. Chen¹⁰⁷ B. Chen¹⁵² B. Chen¹⁶⁶
 H. Chen^{14c} H. Chen²⁹ J. Chen^{62c} J. Chen¹⁴³ M. Chen¹²⁷ S. Chen¹⁵⁴ S. J. Chen^{14c} X. Chen^{62c,136}
 X. Chen^{14b,l} Y. Chen^{62a} C. L. Cheng¹⁷¹ H. C. Cheng^{64a} S. Cheong¹⁴⁴ A. Cheplakov³⁸ E. Cheremushkina⁴⁸
 E. Cherepanova¹¹⁵ R. Cherkaoui El Moursli^{35e} E. Cheu⁷ K. Cheung⁶⁵ L. Chevalier¹³⁶ V. Chiarella⁵³
 G. Chiarelli^{74a} N. Chiedde¹⁰³ G. Chiodini^{70a} A. S. Chisholm²⁰ A. Chitan^{27b} M. Chitishvili¹⁶⁴
 M. V. Chizhov³⁸ K. Choi¹¹ Y. Chou¹³⁹ E. Y. S. Chow¹¹⁴ K. L. Chu¹⁷⁰ M. C. Chu^{64a} X. Chu^{14a,14e}
 J. Chudoba¹³² J. J. Chwastowski⁸⁷ D. Cieri¹¹¹ K. M. Ciesla^{86a} V. Cindro⁹⁴ A. Ciocio^{17a} F. Cirotto^{72a,72b}
 Z. H. Citron¹⁷⁰ M. Citterio^{71a} D. A. Ciubotaru^{27b} A. Clark⁵⁶ P. J. Clark⁵² C. Clarry¹⁵⁶
 J. M. Clavijo Columbie⁴⁸ S. E. Clawson⁴⁸ C. Clement^{47a,47b} J. Clercx⁴⁸ Y. Coadou¹⁰³ M. Cobal^{69a,69c}
 A. Cocco^{57b} R. F. Coelho Barrue^{131a} R. Coelho Lopes De Sa¹⁰⁴ S. Coelli^{71a} B. Cole⁴¹ J. Collot⁶⁰
 P. Conde Muiño^{131a,131g} M. P. Connell^{33c} S. H. Connell^{33c} E. I. Conroy¹²⁷ F. Conventi^{72a,m} H. G. Cooke²⁰
 A. M. Cooper-Sarkar¹²⁷ A. Cordeiro Oudot Choi¹²⁸ L. D. Corpe⁴⁰ M. Corradi^{75a,75b} F. Corriveau^{105,n}
 A. Cortes-Gonzalez¹⁸ M. J. Costa¹⁶⁴ F. Costanza⁴ D. Costanzo¹⁴⁰ B. M. Cote¹²⁰ G. Cowan⁹⁶ K. Cranmer¹⁷¹
 D. Cremonini^{23b,23a} S. Crépe-Renaudin⁶⁰ F. Crescioli¹²⁸ M. Cristinziani¹⁴² M. Cristoforetti^{78a,78b} V. Croft¹¹⁵
 J. E. Crosby¹²² G. Crossetti^{43b,43a} A. Cueto¹⁰⁰ H. Cui^{14a,14e} Z. Cui⁷ W. R. Cunningham⁵⁹ F. Curcio¹⁶⁴
 J. R. Curran⁵² P. Czodrowski³⁶ M. M. Czurylo³⁶ M. J. Da Cunha Sargedas De Sousa^{57b,57a}
 J. V. Da Fonseca Pinto^{83b} C. Da Via¹⁰² W. Dabrowski^{86a} T. Dado⁴⁹ S. Dahbi¹⁴⁹ T. Dai¹⁰⁷ D. Dal Santo¹⁹
 C. Dallapiccola¹⁰⁴ M. Dam⁴² G. D'amen²⁹ V. D'Amico¹¹⁰ J. Damp¹⁰¹ J. R. Dandoy³⁴ M. Danninger¹⁴³
 V. Dao³⁶ G. Darbo^{57b} S. J. Das^{29,o} F. Dattola⁴⁸ S. D'Auria^{71a,71b} A. D'Avanzo^{72a,72b} C. David^{33a}
 T. Davidek¹³⁴ B. Davis-Purcell³⁴ I. Dawson⁹⁵ H. A. Day-hall¹³³ K. De⁸ R. De Asmundis^{72a} N. De Biase⁴⁸
 S. De Castro^{23b,23a} N. De Groot¹¹⁴ P. de Jong¹¹⁵ H. De la Torre¹¹⁶ A. De Maria^{14c} A. De Salvo^{75a}
 U. De Sanctis^{76a,76b} F. De Santis^{70a,70b} A. De Santo¹⁴⁷ J. B. De Vivie De Regie⁶⁰ D. V. Dedovich³⁸ J. Degen⁹³
 A. M. Deiana⁴⁴ F. Del Corso^{23b,23a} J. Del Peso¹⁰⁰ F. Del Rio^{63a} L. Delagrangé¹²⁸ F. Deliot¹³⁶
 C. M. Delitzsch⁴⁹ M. Della Pietra^{72a,72b} D. Della Volpe⁵⁶ A. Dell'Acqua³⁶ L. Dell'Asta^{71a,71b} M. Delmastro⁴
 P. A. Delsart⁶⁰ S. Demers¹⁷³ M. Demichev³⁸ S. P. Denisov³⁷ L. D'Eramo⁴⁰ D. Derendarz⁸⁷ F. Derue¹²⁸
 P. Dervan⁹³ K. Desch²⁴ C. Deutsch²⁴ F. A. Di Bello^{57b,57a} A. Di Ciaccio^{76a,76b} L. Di Ciaccio⁴
 A. Di Domenico^{75a,75b} C. Di Donato^{72a,72b} A. Di Girolamo³⁶ G. Di Gregorio³⁶ A. Di Luca^{78a,78b}
 B. Di Micco^{77a,77b} R. Di Nardo^{77a,77b} M. Diamantopoulou³⁴ F. A. Dias¹¹⁵ T. Dias Do Vale¹⁴³
 M. A. Diaz^{138a,138b} F. G. Diaz Capriles²⁴ M. Didenko¹⁶⁴ E. B. Diehl¹⁰⁷ S. Díez Cornell⁴⁸ C. Díez Pardos¹⁴²
 C. Dimitriadi^{162,24} A. Dimitrievska²⁰ J. Dingfelder²⁴ I-M. Dinu^{27b} S. J. Dittmeier^{63b} F. Dittus³⁶
 M. Divisek¹³⁴ F. Djama¹⁰³ T. Djobava^{150b} C. Doglioni^{102,99} A. Dohnalova^{28a} J. Dolejsi¹³⁴ Z. Dolezal¹³⁴

K. M. Dona³⁹ M. Donadelli^{83c} B. Dong¹⁰⁸ J. Donini⁴⁰ A. D'Onofrio^{72a,72b} M. D'Onofrio⁹³ J. Dopke¹³⁵
 A. Doria^{72a} N. Dos Santos Fernandes^{131a} P. Dougan¹⁰² M. T. Dova⁹¹ A. T. Doyle⁵⁹ M. A. Draguet¹²⁷
 E. Dreyer¹⁷⁰ I. Drivas-koulouris¹⁰ M. Drnević¹¹⁸ M. Drozdova⁵⁶ D. Du^{62a} T. A. du Pree¹¹⁵ F. Dubinin³⁷
 M. Dubovsky^{28a} E. Duchovni¹⁷⁰ G. Duckeck¹¹⁰ O. A. Ducu^{27b} D. Duda⁵² A. Dudarev³⁶ E. R. Duden²⁶
 M. D'uffizi¹⁰² L. Dufлот⁶⁶ M. Dührssen³⁶ I. Duminica^{27g} A. E. Dumitriu^{27b} M. Dunford^{63a} S. Dungs⁴⁹
 K. Dunne^{47a,47b} A. Duperrin¹⁰³ H. Duran Yildiz^{3a} M. Düren⁵⁸ A. Durglishvili^{150b} B. L. Dwyer¹¹⁶
 G. I. Dyckes^{17a} M. Dyndal^{86a} B. S. Dziedzic⁸⁷ Z. O. Earnshaw¹⁴⁷ G. H. Eberwein¹²⁷ B. Eckerova^{28a}
 S. Eggebrecht⁵⁵ E. Egidio Purcino De Souza¹²⁸ L. F. Ehrke⁵⁶ G. Eigen¹⁶ K. Einsweiler^{17a} T. Ekelof¹⁶²
 P. A. Ekman⁹⁹ S. El Farkh^{35b} Y. El Ghazali^{35b} H. El Jarrari³⁶ A. El Moussaouy¹⁰⁹ V. Ellajosyula¹⁶²
 M. Ellert¹⁶² F. Ellinghaus¹⁷² N. Ellis³⁶ J. Elmsheuser²⁹ M. Elsayw^{117a} M. Elsing³⁶ D. Emelianov¹³⁵
 Y. Enari¹⁵⁴ I. Ene^{17a} S. Epari¹³ P. A. Erland⁸⁷ M. Errenst¹⁷² M. Escalier⁶⁶ C. Escobar¹⁶⁴ E. Etzion¹⁵²
 G. Evans^{131a} H. Evans⁶⁸ L. S. Evans⁹⁶ A. Ezhilov³⁷ S. Ezzarqtouni^{35a} F. Fabbri^{23b,23a} L. Fabbri^{23b,23a}
 G. Facini⁹⁷ V. Fadeyev¹³⁷ R. M. Fakhrtudinov³⁷ D. Fakoudis¹⁰¹ S. Falciano^{75a} L. F. Falda Ulhoa Coelho³⁶
 P. J. Falke²⁴ F. Fallavollita¹¹¹ J. Faltova¹³⁴ C. Fan¹⁶³ Y. Fan^{14a} Y. Fang^{14a,14c} M. Fanti^{71a,71b} M. Faraj^{69a,69b}
 Z. Farazpay⁹⁸ A. Farbin⁸ A. Farilla^{77a} T. Farooque¹⁰⁸ S. M. Farrington⁵² F. Fassi^{35e} D. Fassouliotis⁹
 M. Faucci Giannelli^{76a,76b} W. J. Fawcett³² L. Fayard⁶⁶ P. Federic¹³⁴ P. Federicova¹³² O. L. Fedin^{37,k}
 M. Feickert¹⁷¹ L. Felgioni¹⁰³ D. E. Fellers¹²⁴ C. Feng^{62b} M. Feng^{14b} Z. Feng¹¹⁵ M. J. Fenton¹⁶⁰
 L. Ferencz⁴⁸ R. A. M. Ferguson⁹² S. I. Fernandez Luengo^{138f} P. Fernandez Martinez¹³ M. J. V. Fernoux¹⁰³
 J. Ferrando⁹² A. Ferrari¹⁶² P. Ferrari^{115,114} R. Ferrari^{73a} D. Ferrere⁵⁶ C. Ferretti¹⁰⁷ F. Fiedler¹⁰¹
 P. Fiedler¹³³ A. Filipčić⁹⁴ E. K. Filmer¹ F. Filthaut¹¹⁴ M. C. N. Fiolhais^{131a,131c,p} L. Fiorini¹⁶⁴
 W. C. Fisher¹⁰⁸ T. Fitschen¹⁰² P. M. Fitzhugh¹³⁶ I. Fleck¹⁴² P. Fleischmann¹⁰⁷ T. Flick¹⁷² M. Flores^{33d,q}
 L. R. Flores Castillo^{64a} L. Flores Sanz De Acedo³⁶ F. M. Follega^{78a,78b} N. Fomin¹⁶ J. H. Foo¹⁵⁶ A. Formica¹³⁶
 A. C. Forti¹⁰² E. Fortin³⁶ A. W. Fortman^{17a} M. G. Foti^{17a} L. Fountas^{9,r} D. Fournier⁶⁶ H. Fox⁹²
 P. Francavilla^{74a,74b} S. Francescato⁶¹ S. Franchellucci⁵⁶ M. Franchini^{23b,23a} S. Franchino^{63a} D. Francis³⁶
 L. Franco¹¹⁴ V. Franco Lima³⁶ L. Franconi⁴⁸ M. Franklin⁶¹ G. Frattari²⁶ W. S. Freund^{83b} Y. Y. Frid¹⁵²
 J. Friend⁵⁹ N. Fritzsche⁵⁰ A. Froch⁵⁴ D. Froidevaux³⁶ J. A. Frost¹²⁷ Y. Fu^{62a} S. Fuenzalida Garrido^{138f}
 M. Fujimoto¹⁰³ K. Y. Fung^{64a} E. Furtado De Simas Filho^{83e} M. Furukawa¹⁵⁴ J. Fuster¹⁶⁴ A. Gabrielli^{23b,23a}
 A. Gabrielli¹⁵⁶ P. Gadow³⁶ G. Gagliardi^{57b,57a} L. G. Gagnon^{17a} S. Galantzan¹⁵² E. J. Gallas¹²⁷
 B. J. Gallop¹³⁵ K. K. Gan¹²⁰ S. Ganguly¹⁵⁴ Y. Gao⁵² F. M. Garay Walls^{138a,138b} B. Garcia²⁹ C. García¹⁶⁴
 A. Garcia Alonso¹¹⁵ A. G. Garcia Caffaro¹⁷³ J. E. García Navarro¹⁶⁴ M. Garcia-Sciveres^{17a} G. L. Gardner¹²⁹
 R. W. Gardner³⁹ N. Garelli¹⁵⁹ D. Garg⁸⁰ R. B. Garg^{144,s} J. M. Gargan⁵² C. A. Garner¹⁵⁶ C. M. Garvey^{33a}
 P. Gaspar^{83b} V. K. Gassmann¹⁵⁹ G. Gaudio^{73a} V. Gautam¹³ P. Gauzzi^{75a,75b} I. L. Gavrilenko³⁷ A. Gavrilyuk³⁷
 C. Gay¹⁶⁵ G. Gaycken⁴⁸ E. N. Gazis¹⁰ A. A. Geanta^{27b} C. M. Gee¹³⁷ A. Gekow¹²⁰ C. Gemme^{57b}
 M. H. Genest⁶⁰ A. D. Gentry¹¹³ S. George⁹⁶ W. F. George²⁰ T. Geralis⁴⁶ P. Gessinger-Befurt³⁶
 M. E. Geyik¹⁷² M. Ghani¹⁶⁸ K. Ghorbanian⁹⁵ A. Ghosal¹⁴² A. Ghosh¹⁶⁰ A. Ghosh⁷ B. Giacobbe^{23b}
 S. Giagu^{75a,75b} T. Giani¹¹⁵ P. Giannetti^{74a} A. Giannini^{62a} S. M. Gibson⁹⁶ M. Gignac¹³⁷ D. T. Gil^{86b}
 A. K. Gilbert^{86a} B. J. Gilbert⁴¹ D. Gillberg³⁴ G. Gilles¹¹⁵ L. Ginabat¹²⁸ D. M. Gingrich^{2,e}
 M. P. Giordani^{69a,69c} P. F. Giraud¹³⁶ G. Giugliarelli^{69a,69c} D. Giugni^{71a} F. Giuli³⁶ I. Gkialas^{9,r}
 L. K. Gladilin³⁷ C. Glasman¹⁰⁰ G. R. Gledhill¹²⁴ G. Glemža⁴⁸ M. Glisic¹²⁴ I. Gnesi^{43b,t} Y. Go²⁹
 M. Goblirsch-Kolb³⁶ B. Gocke⁴⁹ D. Godin¹⁰⁹ B. Gokturk^{21a} S. Goldfarb¹⁰⁶ T. Golling⁵⁶ M. G. D. Gololo^{33g}
 D. Golubkov³⁷ J. P. Gombas¹⁰⁸ A. Gomes^{131a,131b} G. Gomes Da Silva¹⁴² A. J. Gomez Delegido¹⁶⁴
 R. Gonçalves^{131a,131c} L. Gonella²⁰ A. Gongadze^{150c} F. Gonnella²⁰ J. L. Gonski¹⁴⁴ R. Y. González Andana¹⁵²
 S. González de la Hoz¹⁶⁴ R. Gonzalez Lopez⁹³ C. Gonzalez Renteria^{17a} M. V. Gonzalez Rodrigues⁴⁸
 R. Gonzalez Suarez¹⁶² S. Gonzalez-Sevilla⁵⁶ L. Goossens³⁶ B. Gorini³⁶ E. Gorini^{70a,70b} A. Gorišek⁹⁴
 T. C. Gosart¹²⁹ A. T. Goshaw⁵¹ M. I. Gostkin³⁸ S. Goswami¹²² C. A. Gottardo³⁶ S. A. Gotz¹¹⁰
 M. Goughri^{35b} V. Goumarre⁴⁸ A. G. Goussiou¹³⁹ N. Govender^{33c} I. Grabowska-Bold^{86a} K. Graham³⁴
 E. Gramstad¹²⁶ S. Grancagnolo^{70a,70b} C. M. Grant^{1,136} P. M. Gravila^{27f} F. G. Gravili^{70a,70b} H. M. Gray^{17a}
 M. Greco^{70a,70b} C. Greife²⁴ I. M. Gregor⁴⁸ K. T. Greif¹⁶⁰ P. Grenier¹⁴⁴ S. G. Grewe¹¹¹ A. A. Grillo¹³⁷
 K. Grimm³¹ S. Grinstein^{13,u} J.-F. Grivaz⁶⁶ E. Gross¹⁷⁰ J. Grosse-Knetter⁵⁵ J. C. Grundy¹²⁷ L. Guan¹⁰⁷

C. Gubbels¹⁶⁵ J. G. R. Guerrero Rojas¹⁶⁴ G. Guerrieri^{69a,69c} F. Guescini¹¹¹ R. Gugel¹⁰¹ J. A. M. Guhit¹⁰⁷
A. Guida¹⁸ E. Guilloton¹⁶⁸ S. Guindon³⁶ F. Guo^{14a,14e} J. Guo^{62c} L. Guo⁴⁸ Y. Guo¹⁰⁷ R. Gupta⁴⁸
R. Gupta¹³⁰ S. Gurbuz²⁴ S. S. Gurdasani⁵⁴ G. Gustavino³⁶ M. Guth⁵⁶ P. Gutierrez¹²¹
L. F. Gutierrez Zagazeta¹²⁹ M. Gutsche⁵⁰ C. Gutschow⁹⁷ C. Gwenlan¹²⁷ C. B. Gwilliam⁹³ E. S. Haaland¹²⁶
A. Haas¹¹⁸ M. Habedank⁴⁸ C. Haber^{17a} H. K. Hadavand⁸ A. Hadeef⁵⁰ S. Hadzic¹¹¹ A. I. Hagan⁹²
J. J. Hahn¹⁴² E. H. Haines⁹⁷ M. Haleem¹⁶⁷ J. Haley¹²² J. J. Hall¹⁴⁰ G. D. Hallowell¹⁰³ L. Halser¹⁹
K. Hamano¹⁶⁶ M. Hamer²⁴ G. N. Hamity⁵² E. J. Hampshire⁹⁶ J. Han^{62b} K. Han^{62a} L. Han^{14c} L. Han^{62a}
S. Han^{17a} Y. F. Han¹⁵⁶ K. Hanagaki⁸⁴ M. Hance¹³⁷ D. A. Hangal⁴¹ H. Hanif¹⁴³ M. D. Hank¹²⁹
J. B. Hansen⁴² P. H. Hansen⁴² K. Hara¹⁵⁸ D. Harada⁵⁶ T. Harenberg¹⁷² S. Harkusha³⁷ M. L. Harris¹⁰⁴
Y. T. Harris¹²⁷ J. Harrison¹³ N. M. Harrison¹²⁰ P. F. Harrison¹⁶⁸ N. M. Hartman¹¹¹ N. M. Hartmann¹¹⁰
Y. Hasegawa¹⁴¹ S. Hassan¹⁶ R. Hauser¹⁰⁸ C. M. Hawkes²⁰ R. J. Hawkings³⁶ Y. Hayashi¹⁵⁴ S. Hayashida¹¹²
D. Hayden¹⁰⁸ C. Hayes¹⁰⁷ R. L. Hayes¹¹⁵ C. P. Hays¹²⁷ J. M. Hays⁹⁵ H. S. Hayward⁹³ F. He^{62a}
M. He^{14a,14e} Y. He¹⁵⁵ Y. He⁴⁸ Y. He⁹⁷ N. B. Heatley⁹⁵ V. Hedberg⁹⁹ A. L. Heggelund¹²⁶ N. D. Hehir^{95,a}
C. Heidegger⁵⁴ K. K. Heidegger⁵⁴ W. D. Heidorn⁸¹ J. Heilman³⁴ S. Heim⁴⁸ T. Heim^{17a} J. G. Heinlein¹²⁹
J. J. Heinrich¹²⁴ L. Heinrich^{111,v} J. Hejbal¹³² A. Held¹⁷¹ S. Hellesund¹⁶ C. M. Helling¹⁶⁵ S. Hellman^{47a,47b}
R. C. W. Henderson⁹² L. Henkelmann³² A. M. Henriques Correia³⁶ H. Herde⁹⁹ Y. Hernández Jiménez¹⁴⁶
L. M. Herrmann²⁴ T. Herrmann⁵⁰ G. Herten⁵⁴ R. Hertenberger¹¹⁰ L. Hervas³⁶ M. E. Hesping¹⁰¹
N. P. Hessey^{157a} E. Hill¹⁵⁶ S. J. Hillier²⁰ J. R. Hinds¹⁰⁸ F. Hinterkeuser²⁴ M. Hirose¹²⁵ S. Hirose¹⁵⁸
D. Hirschbuehl¹⁷² T. G. Hitchings¹⁰² B. Hiti⁹⁴ J. Hobbs¹⁴⁶ R. Hobincu^{27e} N. Hod¹⁷⁰ M. C. Hodgkinson¹⁴⁰
B. H. Hodgkinson¹²⁷ A. Hoecker³⁶ D. D. Hofer¹⁰⁷ J. Hofer⁴⁸ T. Holm²⁴ M. Holzbock¹¹¹
L. B. A. H. Hommels³² B. P. Honan¹⁰² J. Hong^{62c} T. M. Hong¹³⁰ B. H. Hooberman¹⁶³ W. H. Hopkins⁶
Y. Horii¹¹² S. Hou¹⁴⁹ A. S. Howard⁹⁴ J. Howarth⁵⁹ J. Hoya⁶ M. Hrabovsky¹²³ A. Hrynevich⁴⁸
T. Hryn'ova⁴ P. J. Hsu⁶⁵ S.-C. Hsu¹³⁹ M. Hu^{17a} Q. Hu^{62a} S. Huang^{64b} X. Huang^{14a,14e} Y. Huang¹⁴⁰
Y. Huang^{14a} Z. Huang¹⁰² Z. Hubacek¹³³ M. Huebner²⁴ F. Huegging²⁴ T. B. Huffman¹²⁷ C. A. Hugli⁴⁸
M. Huhtinen³⁶ S. K. Huiberts¹⁶ R. Hulsken¹⁰⁵ N. Huseynov¹² J. Huston¹⁰⁸ J. Huth⁶¹ R. Hyneman¹⁴⁴
G. Iacobucci⁵⁶ G. Iakovidis²⁹ I. Ibragimov¹⁴² L. Iconomidou-Fayard⁶⁶ J. P. Iddon³⁶ P. Iengo^{72a,72b}
R. Iguchi¹⁵⁴ T. Iizawa¹²⁷ Y. Ikegami⁸⁴ N. Ilic¹⁵⁶ H. Imam^{35a} M. Ince Lezki⁵⁶ T. Ingebretsen Carlson^{47a,47b}
G. Introzzi^{73a,73b} M. Iodice^{77a} V. Ippolito^{75a,75b} R. K. Irwin⁹³ M. Ishino¹⁵⁴ W. Islam¹⁷¹ C. Issever^{18,48}
S. Istin^{21a,w} H. Ito¹⁶⁹ R. Iuppa^{78a,78b} A. Ivina¹⁷⁰ J. M. Izen⁴⁵ V. Izzo^{72a} P. Jacka^{132,133} P. Jackson¹
B. P. Jaeger¹⁴³ C. S. Jagfeld¹¹⁰ G. Jain^{157a} P. Jain⁵⁴ K. Jakobs⁵⁴ T. Jakoubek¹⁷⁰ J. Jamieson⁵⁹
K. W. Janas^{86a} M. Javurkova¹⁰⁴ L. Jeanty¹²⁴ J. Jejelava^{150a,x} P. Jenni^{54,y} C. E. Jessiman³⁴ C. Jia^{62b} J. Jia¹⁴⁶
X. Jia⁶¹ X. Jia^{14a,14e} Z. Jia^{14c} C. Jiang⁵² S. Jiggins⁴⁸ J. Jimenez Pena¹³ S. Jin^{14c} A. Jinaru^{27b}
O. Jinnouchi¹⁵⁵ P. Johansson¹⁴⁰ K. A. Johns⁷ J. W. Johnson¹³⁷ D. M. Jones¹⁴⁷ E. Jones⁴⁸ P. Jones³²
R. W. L. Jones⁹² T. J. Jones⁹³ H. L. Joos^{55,36} R. Joshi¹²⁰ J. Jovicevic¹⁵ X. Ju^{17a} J. J. Junggeburth¹⁰⁴
T. Junkermann^{63a} A. Juste Rozas^{13,u} M. K. Juzek⁸⁷ S. Kabana^{138e} A. Kaczmarzka⁸⁷ M. Kado¹¹¹
H. Kagan¹²⁰ M. Kagan¹⁴⁴ A. Kahn⁴¹ A. Kahn¹²⁹ C. Kahra¹⁰¹ T. Kaji¹⁵⁴ E. Kajomovitz¹⁵¹ N. Kakati¹⁷⁰
I. Kalaitzidou⁵⁴ C. W. Kalderon²⁹ N. J. Kang¹³⁷ D. Kar^{33g} K. Karava¹²⁷ M. J. Kareem^{157b} E. Karentzos⁵⁴
I. Karkania¹⁵³ O. Karkout¹¹⁵ S. N. Karpov³⁸ Z. M. Karpova³⁸ V. Kartvelishvili⁹² A. N. Karyukhin³⁷
E. Kasimi¹⁵³ J. Katzy⁴⁸ S. Kaur³⁴ K. Kawade¹⁴¹ M. P. Kawale¹²¹ C. Kawamoto⁸⁸ T. Kawamoto^{62a}
E. F. Kay³⁶ F. I. Kaya¹⁵⁹ S. Kazakos¹⁰⁸ V. F. Kazanin³⁷ Y. Ke¹⁴⁶ J. M. Keaveney^{33a} R. Keeler¹⁶⁶
G. V. Kehris⁶¹ J. S. Keller³⁴ A. S. Kelly⁹⁷ J. J. Kempster¹⁴⁷ P. D. Kennedy¹⁰¹ O. Kepka¹³² B. P. Kerridge¹³⁵
S. Kersten¹⁷² B. P. Kerševan⁹⁴ L. Keszeghova^{28a} S. Ketabchi Haghghat¹⁵⁶ R. A. Khan¹³⁰ A. Khanov¹²²
A. G. Kharlamov³⁷ T. Kharlamova³⁷ E. E. Khoda¹³⁹ M. Kholodenko³⁷ T. J. Khoo¹⁸ G. Khorialiuli¹⁶⁷
J. Khubua^{150b} Y. A. R. Khwaira⁶⁶ B. Kibirige^{33g} A. Kilgallon¹²⁴ D. W. Kim^{47a,47b} Y. K. Kim³⁹ N. Kimura⁹⁷
M. K. Kingston⁵⁵ A. Kirchhoff⁵⁵ C. Kirfel²⁴ F. Kirfel²⁴ J. Kirk¹³⁵ A. E. Kiryunin¹¹¹ C. Kitsaki¹⁰
O. Kivernyk²⁴ M. Klassen¹⁵⁹ C. Klein³⁴ L. Klein¹⁶⁷ M. H. Klein⁴⁴ S. B. Klein⁵⁶ U. Klein⁹³ P. Klimek³⁶
A. Klimentov²⁹ T. Klioutchnikova³⁶ P. Kluit¹¹⁵ S. Kluth¹¹¹ E. Kneringer⁷⁹ T. M. Knight¹⁵⁶ A. Knue⁴⁹
R. Kobayashi⁸⁸ D. Kobylanski¹⁷⁰ S. F. Koch¹²⁷ M. Kocian¹⁴⁴ P. Kodyš¹³⁴ D. M. Koeck¹²⁴ P. T. Koenig²⁴
T. Koffas³⁴ O. Kolay⁵⁰ I. Koletsou⁴ T. Komarek¹²³ K. Köneke⁵⁴ A. X. Y. Kong¹ T. Kono¹¹⁹

N. Konstantinidis⁹⁷ P. Kontaxakis⁵⁶ B. Konya⁹⁹ R. Kopeliainsky⁴¹ S. Koperny^{86a} K. Korcyl⁸⁷ K. Kordas^{153,z}
 A. Korn⁹⁷ S. Korn⁵⁵ I. Korolkov¹³ N. Korotkova³⁷ B. Kortman¹¹⁵ O. Kortner¹¹¹ S. Kortner¹¹¹
 W. H. Kostecka¹¹⁶ V. V. Kostyukhin¹⁴² A. Kotsokechagia¹³⁶ A. Kotwal⁵¹ A. Koulouris³⁶
 A. Kourkoumeli-Charalampidi^{73a,73b} C. Kourkoumelis⁹ E. Kourlitis^{111,v} O. Kovanda¹²⁴ R. Kowalewski¹⁶⁶
 W. Kozanecki¹³⁶ A. S. Kozhin³⁷ V. A. Kramarenko³⁷ G. Kramberger⁹⁴ P. Kramer¹⁰¹ M. W. Krasny¹²⁸
 A. Krasznahorkay³⁶ J. W. Kraus¹⁷² J. A. Kremer⁴⁸ T. Kresse⁵⁰ J. Kretzschmar⁹³ K. Kreul¹⁸ P. Krieger¹⁵⁶
 S. Krishnamurthy¹⁰⁴ M. Krivos¹³⁴ K. Krizka²⁰ K. Kroeninger⁴⁹ H. Kroha¹¹¹ J. Kroll¹³² J. Kroll¹²⁹
 K. S. Krowpman¹⁰⁸ U. Kruchonak³⁸ H. Krüger²⁴ N. Krumnack⁸¹ M. C. Kruse⁵¹ O. Kuchinskaia³⁷ S. Kuday^{3a}
 S. Kuehn³⁶ R. Kuesters⁵⁴ T. Kuhl⁴⁸ V. Kukhtin³⁸ Y. Kulchitsky^{37,k} S. Kuleshov^{138d,138b} M. Kumar^{33g}
 N. Kumari⁴⁸ P. Kumari^{157b} A. Kupco¹³² T. Kupfer⁴⁹ A. Kupich³⁷ O. Kuprash⁵⁴ H. Kurashige⁸⁵
 L. L. Kurchaninov^{157a} O. Kurdysh⁶⁶ Y. A. Kurochkin³⁷ A. Kurova³⁷ M. Kuze¹⁵⁵ A. K. Kvam¹⁰⁴ J. Kvita¹²³
 T. Kwan¹⁰⁵ N. G. Kyriacou¹⁰⁷ L. A. O. Laatu¹⁰³ C. Lacasta¹⁶⁴ F. Lacava^{75a,75b} H. Lacker¹⁸ D. Lacour¹²⁸
 N. N. Lad⁹⁷ E. Ladygin³⁸ A. Lafarge⁴⁰ B. Laforge¹²⁸ T. Lagouri¹⁷³ F. Z. Lahbabi^{35a} S. Lai⁵⁵
 I. K. Lakomic^{86a} N. Lalloue⁶⁰ J. E. Lambert¹⁶⁶ S. Lammers⁶⁸ W. Lampl⁷ C. Lampoudis^{153,z}
 G. Lamprinoudis¹⁰¹ A. N. Lancaster¹¹⁶ E. Lançon²⁹ U. Landgraf⁵⁴ M. P. J. Landon⁹⁵ V. S. Lang⁵⁴
 O. K. B. Langrekken¹²⁶ A. J. Lankford¹⁶⁰ F. Lanni³⁶ K. Lantzsch²⁴ A. Lanza^{73a} A. Lapertosa^{57b,57a}
 J. F. Laporte¹³⁶ T. Lari^{71a} F. Lasagni Manghi^{23b} M. Lassnig³⁶ V. Latonova¹³² A. Laudrain¹⁰¹ A. Laurier¹⁵¹
 S. D. Lawlor¹⁴⁰ Z. Lawrence¹⁰² R. Lazaridou¹⁶⁸ M. Lazzaroni^{71a,71b} B. Le¹⁰² E. M. Le Boulicaut⁵¹
 L. T. Le Pottier^{17a} B. Leban^{23b,23a} A. Lebedev⁸¹ M. LeBlanc¹⁰² F. Ledroit-Guillon⁶⁰ A. C. A. Lee⁹⁷
 S. C. Lee¹⁴⁹ S. Lee^{47a,47b} T. F. Lee⁹³ L. L. Leeuw^{33c} H. P. Lefebvre⁹⁶ M. Lefebvre¹⁶⁶ C. Leggett^{17a}
 G. Lehmann Miotto³⁶ M. Leigh⁵⁶ W. A. Leight¹⁰⁴ W. Leinonen¹¹⁴ A. Leisos^{153,aa} M. A. L. Leite^{83c}
 C. E. Leitgeb¹⁸ R. Leitner¹³⁴ K. J. C. Leney⁴⁴ T. Lenz²⁴ S. Leone^{74a} C. Leonidopoulos⁵² A. Leopold¹⁴⁵
 C. Leroy¹⁰⁹ R. Les¹⁰⁸ C. G. Lester³² M. Levchenko³⁷ J. Levêque⁴ L. J. Levinson¹⁷⁰ G. Levrini^{23b,23a}
 M. P. Lewicki⁸⁷ C. Lewis¹³⁹ D. J. Lewis⁴ A. Li⁵ B. Li^{62b} C. Li^{62a} C-Q. Li¹¹¹ H. Li^{62a} H. Li^{62b} H. Li^{14c}
 H. Li^{14b} H. Li^{62b} J. Li^{62c} K. Li¹³⁹ L. Li^{62c} M. Li^{14a,14e} Q. Y. Li^{62a} S. Li^{14a,14e} S. Li^{62d,62c,bb} T. Li⁵
 X. Li¹⁰⁵ Z. Li¹²⁷ Z. Li¹⁰⁵ Z. Li^{14a,14e} S. Liang^{14a,14e} Z. Liang^{14a} M. Liberatore¹³⁶ B. Liberti^{76a} K. Lie^{64c}
 J. Lieber Marin^{83e} H. Lien⁶⁸ K. Lin¹⁰⁸ R. E. Lindley⁷ J. H. Lindon² E. Lipeles¹²⁹ A. Lipniacka¹⁶
 A. Lister¹⁶⁵ J. D. Little⁴ B. Liu^{14a} B. X. Liu¹⁴³ D. Liu^{62d,62c} E. H. L. Liu²⁰ J. B. Liu^{62a} J. K. K. Liu³²
 K. Liu^{62d} K. Liu^{62d,62c} M. Liu^{62a} M. Y. Liu^{62a} P. Liu^{14a} Q. Liu^{62d,139,62c} X. Liu^{62a} X. Liu^{62b} Y. Liu^{14d,14e}
 Y. L. Liu^{62b} Y. W. Liu^{62a} J. Llorente Merino¹⁴³ S. L. Lloyd⁹⁵ E. M. Lobodzinska⁴⁸ P. Loch⁷ T. Lohse¹⁸
 K. Lohwasser¹⁴⁰ E. Loiacono⁴⁸ M. Lokajicek^{132,a} J. D. Lomas²⁰ J. D. Long¹⁶³ I. Longarini¹⁶⁰
 L. Longo^{70a,70b} R. Longo¹⁶³ I. Lopez Paz⁶⁷ A. Lopez Solis⁴⁸ N. Lorenzo Martinez⁴ A. M. Lory¹¹⁰
 G. Lösche Centeno¹⁴⁷ O. Loseva³⁷ X. Lou^{47a,47b} X. Lou^{14a,14e} A. Lounis⁶⁶ P. A. Love⁹² G. Lu^{14a,14e}
 M. Lu⁶⁶ S. Lu¹²⁹ Y. J. Lu⁶⁵ H. J. Lubatti¹³⁹ C. Luci^{75a,75b} F. L. Lucio Alves^{14c} F. Luehring⁶⁸ I. Luise¹⁴⁶
 O. Lukianchuk⁶⁶ O. Lundberg¹⁴⁵ B. Lund-Jensen¹⁴⁵ N. A. Luongo⁶ M. S. Lutz³⁶ A. B. Lux²⁵ D. Lynn²⁹
 R. Lysak¹³² E. Lytken⁹⁹ V. Lyubushkin³⁸ T. Lyubushkina³⁸ M. M. Lyukova¹⁴⁶ M. Firdaus M. Soberi⁵²
 H. Ma²⁹ K. Ma^{62a} L. L. Ma^{62b} W. Ma^{62a} Y. Ma¹²² D. M. Mac Donell¹⁶⁶ G. Maccarrone⁵³
 J. C. MacDonald¹⁰¹ P. C. Machado De Abreu Farias^{83e} R. Madar⁴⁰ T. Madula⁹⁷ J. Maeda⁸⁵ T. Maeno²⁹
 H. Maguire¹⁴⁰ V. Maiboroda¹³⁶ A. Maio^{131a,131b,131d} K. Maj^{86a} O. Majersky⁴⁸ S. Majewski¹²⁴ N. Makovec⁶⁶
 V. Maksimovic¹⁵ B. Malaescu¹²⁸ Pa. Malecki⁸⁷ V. P. Maleev³⁷ F. Malek^{60,cc} M. Mali⁹⁴ D. Malito⁹⁶
 U. Mallik⁸⁰ S. Maltezos¹⁰ S. Malyukov³⁸ J. Mamuzic¹³ G. Mancini⁵³ M. N. Mancini²⁶ G. Manco^{73a,73b}
 J. P. Mandalia⁹⁵ I. Mandić⁹⁴ L. Manhaes de Andrade Filho^{83a} I. M. Maniatis¹⁷⁰ J. Manjarres Ramos⁹⁰
 D. C. Mankad¹⁷⁰ A. Mann¹¹⁰ S. Manzoni³⁶ L. Mao^{62c} X. Mapekula^{33c} A. Marantis^{153,aa} G. Marchiori⁵
 M. Marcisovsky¹³² C. Marcon^{71a} M. Marinescu²⁰ S. Marium⁴⁸ M. Marjanovic¹²¹ M. Markovitch⁶⁶
 E. J. Marshall⁹² Z. Marshall^{17a} S. Marti-Garcia¹⁶⁴ T. A. Martin¹⁶⁸ V. J. Martin⁵² B. Martin dit Latour¹⁶
 L. Martinelli^{75a,75b} M. Martinez^{13,u} P. Martinez Agullo¹⁶⁴ V. I. Martinez Outschoorn¹⁰⁴ P. Martinez Suarez¹³
 S. Martin-Haugh¹³⁵ G. Martinovicova¹³⁴ V. S. Martoiu^{27b} A. C. Martyniuk⁹⁷ A. Marzin³⁶ D. Mascione^{78a,78b}
 L. Masetti¹⁰¹ T. Mashimo¹⁵⁴ J. Masik¹⁰² A. L. Maslennikov³⁷ P. Massarotti^{72a,72b} P. Mastrandrea^{74a,74b}
 A. Mastroberardino^{43b,43a} T. Masubuchi¹⁵⁴ T. Mathisen¹⁶² J. Matousek¹³⁴ N. Matsuzawa¹⁵⁴ J. Maurer^{27b}

A. J. Maury⁶⁶ B. Maček⁹⁴ D. A. Maximov³⁷ A. E. May¹⁰² R. Mazini¹⁴⁹ I. Maznas¹¹⁶ M. Mazza¹⁰⁸
S. M. Mazza¹³⁷ E. Mazzeo^{71a,71b} C. Mc Ginn²⁹ J. P. Mc Gowan¹⁶⁶ S. P. Mc Kee¹⁰⁷ C. C. McCracken¹⁶⁵
E. F. McDonald¹⁰⁶ A. E. McDougall¹¹⁵ J. A. Mcfayden¹⁴⁷ R. P. McGovern¹²⁹ G. Mchedlidze^{150b}
R. P. McKenzie^{33g} T. C. McLachlan⁴⁸ D. J. McLaughlin⁹⁷ S. J. McMahon¹³⁵ C. M. Mcpartland⁹³
R. A. McPherson^{166,n} S. Mehlhase¹¹⁰ A. Mehta⁹³ D. Melini¹⁶⁴ B. R. Mellado Garcia^{33g} A. H. Melo⁵⁵
F. Meloni⁴⁸ A. M. Mendes Jacques Da Costa¹⁰² H. Y. Meng¹⁵⁶ L. Meng⁹² S. Menke¹¹¹ M. Mentink³⁶
E. Meoni^{43b,43a} G. Mercado¹¹⁶ C. Merlassino^{69a,69c} L. Merola^{72a,72b} C. Meroni^{71a,71b} J. Metcalfe⁶
A. S. Mete⁶ C. Meyer⁶⁸ J-P. Meyer¹³⁶ R. P. Middleton¹³⁵ L. Mijović⁵² G. Mikenberg¹⁷⁰ M. Mikestikova¹³²
M. Mikuž⁹⁴ H. Mildner¹⁰¹ A. Milic³⁶ D. W. Miller³⁹ E. H. Miller¹⁴⁴ L. S. Miller³⁴ A. Milov¹⁷⁰
D. A. Milstead^{47a,47b} T. Min^{14c} A. A. Minaenko³⁷ I. A. Minashvili^{150b} L. Mince⁵⁹ A. I. Mincer¹¹⁸ B. Mindur^{86a}
M. Mineev³⁸ Y. Mino⁸⁸ L. M. Mir¹³ M. Miralles Lopez⁵⁹ M. Mironova^{17a} A. Mishima¹⁵⁴ M. C. Missio¹¹⁴
A. Mitra¹⁶⁸ V. A. Mitsou¹⁶⁴ Y. Mitsumori¹¹² O. Miu¹⁵⁶ P. S. Miyagawa⁹⁵ T. Mkrtchyan^{63a} M. Mlinarevic⁹⁷
T. Mlinarevic⁹⁷ M. Mlynarikova³⁶ S. Mobius¹⁹ P. Mogg¹¹⁰ M. H. Mohamed Farook¹¹³ A. F. Mohammed^{14a,14e}
S. Mohapatra⁴¹ G. Mokgatitwane^{33g} L. Moleri¹⁷⁰ B. Mondal¹⁴² S. Mondal¹³³ K. Mönig⁴⁸ E. Monnier¹⁰³
L. Monsonis Romero¹⁶⁴ J. Montejo Berlingen¹³ M. Montella¹²⁰ F. Montereali^{77a,77b} F. Monticelli⁹¹
S. Monzani^{69a,69c} N. Morange⁶⁶ A. L. Moreira De Carvalho⁴⁸ M. Moreno Llácer¹⁶⁴ C. Moreno Martinez⁵⁶
P. Morettini^{57b} S. Morgenstern³⁶ M. Morii⁶¹ M. Morinaga¹⁵⁴ F. Morodei^{75a,75b} L. Morvaj³⁶
P. Moschovakos³⁶ B. Moser³⁶ M. Mosidze^{150b} T. Moskalets⁵⁴ P. Moskvitina¹¹⁴ J. Moss^{31,dd} A. Moussa^{35d}
E. J. W. Moyses¹⁰⁴ O. Mtintsilana^{33g} S. Muanza¹⁰³ J. Mueller¹³⁰ D. Muenstermann⁹² R. Müller¹⁹
G. A. Mullier¹⁶² A. J. Mullin³² J. J. Mullin¹²⁹ D. P. Mungo¹⁵⁶ D. Munoz Perez¹⁶⁴ F. J. Munoz Sanchez¹⁰²
M. Murin¹⁰² W. J. Murray^{168,135} M. Muškinja⁹⁴ C. Mwewa²⁹ A. G. Myagkov^{37,k} A. J. Myers⁸ G. Myers¹⁰⁷
M. Myska¹³³ B. P. Nachman^{17a} O. Nackenhorst⁴⁹ K. Nagai¹²⁷ K. Nagano⁸⁴ J. L. Nagle^{29,o} E. Nagy¹⁰³
A. M. Nairz³⁶ Y. Nakahama⁸⁴ K. Nakamura⁸⁴ K. Nakkalil⁵ H. Nanjo¹²⁵ R. Narayan⁴⁴ E. A. Narayanan¹¹³
I. Naryshkin³⁷ M. Naseri³⁴ S. Nasri^{117b} C. Nass²⁴ G. Navarro^{22a} J. Navarro-Gonzalez¹⁶⁴ R. Nayak¹⁵²
A. Nayaz¹⁸ P. Y. Nechaeva³⁷ F. Nechansky⁴⁸ L. Nedic¹²⁷ T. J. Neep²⁰ A. Negri^{73a,73b} M. Negrini^{23b}
C. Nellist¹¹⁵ C. Nelson¹⁰⁵ K. Nelson¹⁰⁷ S. Nemecek¹³² M. Nessi^{36,ee} M. S. Neubauer¹⁶³ F. Neuhaus¹⁰¹
J. Neundorff⁴⁸ R. Newhouse¹⁶⁵ P. R. Newman²⁰ C. W. Ng¹³⁰ Y. W. Y. Ng⁴⁸ B. Ngair^{117a} H. D. N. Nguyen¹⁰⁹
R. B. Nickerson¹²⁷ R. Nicolaidou¹³⁶ J. Nielsen¹³⁷ M. Niemeyer⁵⁵ J. Niermann⁵⁵ N. Nikiforou³⁶
V. Nikolaenko^{37,k} I. Nikolic-Audit¹²⁸ K. Nikolopoulos²⁰ P. Nilsson²⁹ I. Ninca⁴⁸ H. R. Nindhito⁵⁶
G. Ninio¹⁵² A. Nisati^{75a} N. Nishu² R. Nisius¹¹¹ J-E. Nitschke⁵⁰ E. K. Nkadimeng^{33g} T. Nobe¹⁵⁴
D. L. Noel³² T. Nommensen¹⁴⁸ M. B. Norfolk¹⁴⁰ R. R. B. Norisam⁹⁷ B. J. Norman³⁴ M. Noury^{35a}
J. Novak⁹⁴ T. Novak⁴⁸ L. Novotny¹³³ R. Novotny¹¹³ L. Nozka¹²³ K. Ntekas¹⁶⁰
N. M. J. Nunes De Moura Junior^{83b} J. Ocariz¹²⁸ A. Ochi⁸⁵ I. Ochoa^{131a} S. Oerdek^{48,ff} J. T. Offermann³⁹
A. Ogrodnik¹³⁴ A. Oh¹⁰² C. C. Ohm¹⁴⁵ H. Oide⁸⁴ R. Oishi¹⁵⁴ M. L. Ojeda⁴⁸ Y. Okumura¹⁵⁴
L. F. Oleiro Seabra^{131a} S. A. Olivares Pino^{138d} G. Oliveira Correa¹³ D. Oliveira Damazio²⁹
D. Oliveira Goncalves^{83a} J. L. Oliver¹⁶⁰ Ö. O. Öncel⁵⁴ A. P. O'Neill¹⁹ A. Onofre^{131a,131e} P. U. E. Onyisi¹¹
M. J. Oreglia³⁹ G. E. Orellana⁹¹ D. Orestano^{77a,77b} N. Orlando¹³ R. S. Orr¹⁵⁶ V. O'Shea⁵⁹ L. M. Osojnak¹²⁹
R. Ospanov^{62a} G. Otero y Garzon³⁰ H. Otono⁸⁹ P. S. Ott^{63a} G. J. Ottino^{17a} M. Ouchrif^{35d} F. Ould-Saada¹²⁶
T. Ovsianikova¹³⁹ M. Owen⁵⁹ R. E. Owen¹³⁵ K. Y. Oyulmaz^{21a} V. E. Ozcan^{21a} F. Ozturk⁸⁷ N. Ozturk⁸
S. Ozturk⁸² H. A. Pacey¹²⁷ A. Pacheco Pages¹³ C. Padilla Aranda¹³ G. Padovano^{75a,75b} S. Pagan Griso^{17a}
G. Palacino⁶⁸ A. Palazzo^{70a,70b} J. Pampel²⁴ J. Pan¹⁷³ T. Pan^{64a} D. K. Panchal¹¹ C. E. Pandini¹¹⁵
J. G. Panduro Vazquez⁹⁶ H. D. Pandya¹ H. Pang^{14b} P. Pani⁴⁸ G. Panizzo^{69a,69c} L. Panwar¹²⁸ L. Paolozzi⁵⁶
S. Parajuli¹⁶³ A. Paramonov⁶ C. Paraskevopoulos⁵³ D. Paredes Hernandez^{64b} A. Pareti^{73a,73b} K. R. Park⁴¹
T. H. Park¹⁵⁶ M. A. Parker³² F. Parodi^{57b,57a} E. W. Parrish¹¹⁶ V. A. Parrish⁵² J. A. Parsons⁴¹ U. Parzefall⁵⁴
B. Pascual Dias¹⁰⁹ L. Pascual Dominguez¹⁵² E. Pasqualucci^{75a} S. Passaggio^{57b} F. Pastore⁹⁶ P. Patel⁸⁷
U. M. Patel⁵¹ J. R. Pater¹⁰² T. Pauly³⁶ C. I. Pazos¹⁵⁹ J. Pearkes¹⁴⁴ M. Pedersen¹²⁶ R. Pedro^{131a}
S. V. Peleganchuk³⁷ O. Penc³⁶ E. A. Pender⁵² G. D. Penn¹⁷³ K. E. Penski¹¹⁰ M. Penzin³⁷ B. S. Peralva^{83d}
A. P. Pereira Peixoto¹³⁹ L. Pereira Sanchez¹⁴⁴ D. V. Perepelitsa^{29,o} E. Perez Codina^{157a} M. Perganti¹⁰
H. Pernegger³⁶ O. Perrin⁴⁰ K. Peters⁴⁸ R. F. Y. Peters¹⁰² B. A. Petersen³⁶ T. C. Petersen⁴² E. Petit¹⁰³

V. Petousis¹³³, C. Petridou^{153,z}, T. Petru¹³⁴, A. Petrukhin¹⁴², M. Pettee^{17a}, N. E. Pettersson³⁶, A. Petukhov³⁷, K. Petukhova¹³⁴, R. Pezoa^{138f}, L. Pezzotti³⁶, G. Pezzullo¹⁷³, T. M. Pham¹⁷¹, T. Pham¹⁰⁶, P. W. Phillips¹³⁵, G. Piacquadio¹⁴⁶, E. Pianori^{17a}, F. Piazza¹²⁴, R. Piegaia³⁰, D. Pietreanu^{27b}, A. D. Pilkington¹⁰², M. Pinamonti^{69a,69c}, J. L. Pinfeld², B. C. Pinheiro Pereira^{131a}, A. E. Pinto Pinoargote^{101,136}, L. Pintucci^{69a,69c}, K. M. Piper¹⁴⁷, A. Pirttikoski⁵⁶, D. A. Pizzi³⁴, L. Pizzimento^{64b}, A. Pizzini¹¹⁵, M.-A. Pleier²⁹, V. Plesanovs⁵⁴, V. Pleskot¹³⁴, E. Plotnikova³⁸, G. Poddar⁹⁵, R. Poettgen⁹⁹, L. Poggioli¹²⁸, I. Pokharel⁵⁵, S. Polacek¹³⁴, G. Polesello^{73a}, A. Poley^{143,157a}, A. Polini^{23b}, C. S. Pollard¹⁶⁸, Z. B. Pollock¹²⁰, E. Pompa Pacchi^{75a,75b}, D. Ponomarenko¹¹⁴, L. Pontecorvo³⁶, S. Popa^{27a}, G. A. Popeneciu^{27d}, A. Poreba³⁶, D. M. Portillo Quintero^{157a}, S. Pospisil¹³³, M. A. Postill¹⁴⁰, P. Postolache^{27c}, K. Potamianos¹⁶⁸, P. A. Potepa^{86a}, I. N. Potrap³⁸, C. J. Potter³², H. Potti¹, J. Poveda¹⁶⁴, M. E. Pozo Astigarraga³⁶, A. Prades Ibanez¹⁶⁴, J. Pretel⁵⁴, D. Price¹⁰², M. Primavera^{70a}, M. A. Principe Martin¹⁰⁰, R. Privara¹²³, T. Procter⁵⁹, M. L. Proffitt¹³⁹, N. Proklova¹²⁹, K. Prokofiev^{64c}, G. Proto¹¹¹, J. Proudfoot⁶, M. Przybycien^{86a}, W. W. Przygoda^{86b}, A. Psallidas⁴⁶, J. E. Puddefoot¹⁴⁰, D. Pudzha³⁷, D. Pyatiizbyantseva³⁷, J. Qian¹⁰⁷, D. Qichen¹⁰², Y. Qin¹³, T. Qiu⁵², A. Quadt⁵⁵, M. Queitsch-Maitland¹⁰², G. Quetant⁵⁶, R. P. Quinn¹⁶⁵, G. Rabanal Bolanos⁶¹, D. Rafanoharana⁵⁴, F. Ragusa^{71a,71b}, J. L. Rainbolt³⁹, J. A. Raine⁵⁶, S. Rajagopalan²⁹, E. Ramakoti³⁷, I. A. Ramirez-Berend³⁴, K. Ran^{48,14c}, N. P. Rapheeha^{33g}, H. Rasheed^{27b}, V. Raskina¹²⁸, D. F. Rassloff^{63a}, A. Rastogi^{17a}, S. Rave¹⁰¹, B. Ravina⁵⁵, I. Ravinovich¹⁷⁰, M. Raymond³⁶, A. L. Read¹²⁶, N. P. Readioff¹⁴⁰, D. M. Rebuzzi^{73a,73b}, G. Redlinger²⁹, A. S. Reed¹¹¹, K. Reeves²⁶, J. A. Reidelsturz¹⁷², D. Reikher¹⁵², A. Rej⁴⁹, C. Rembser³⁶, M. Renda^{27b}, M. B. Rendel¹¹¹, F. Renner⁴⁸, A. G. Rennie¹⁶⁰, A. L. Rescia⁴⁸, S. Resconi^{71a}, M. Ressegotti^{57b,57a}, S. Rettie³⁶, J. G. Reyes Rivera¹⁰⁸, E. Reynolds^{17a}, O. L. Rezanova³⁷, P. Reznicek¹³⁴, H. Riani^{35d}, N. Ribaric⁹², E. Ricci^{78a,78b}, R. Richter¹¹¹, S. Richter^{47a,47b}, E. Richter-Was^{86b}, M. Ridel¹²⁸, S. Ridouani^{35d}, P. Rieck¹¹⁸, P. Riedler³⁶, E. M. Riefel^{47a,47b}, J. O. Rieger¹¹⁵, M. Rijssenbeek¹⁴⁶, M. Rimoldi³⁶, L. Rinaldi^{23b,23a}, T. T. Rinn²⁹, M. P. Rinnagel¹¹⁰, G. Ripellino¹⁶², I. Riu¹³, J. C. Rivera Vergara¹⁶⁶, F. Rizatdinova¹²², E. Rizvi⁹⁵, B. R. Roberts^{17a}, S. H. Robertson^{105,n}, D. Robinson³², C. M. Robles Gajardo^{138f}, M. Robles Manzano¹⁰¹, A. Robson⁵⁹, A. Rocchi^{76a,76b}, C. Roda^{74a,74b}, S. Rodriguez Bosca³⁶, Y. Rodriguez Garcia^{22a}, A. Rodriguez Rodriguez⁵⁴, A. M. Rodríguez Vera¹¹⁶, S. Roe³⁶, J. T. Roemer¹⁶⁰, A. R. Roepe-Gier¹³⁷, J. Roggel¹⁷², O. Røhne¹²⁶, R. A. Rojas¹⁰⁴, C. P. A. Roland¹²⁸, J. Roloff²⁹, A. Romaniouk³⁷, E. Romano^{73a,73b}, M. Romano^{23b}, A. C. Romero Hernandez¹⁶³, N. Rompotis⁹³, L. Roos¹²⁸, S. Rosati^{75a}, B. J. Rosser³⁹, E. Rossi¹²⁷, E. Rossi^{72a,72b}, L. P. Rossi⁶¹, L. Rossini⁵⁴, R. Rosten¹²⁰, M. Rotaru^{27b}, B. Rottler⁵⁴, C. Rougier⁹⁰, D. Rousseau⁶⁶, D. Rousso³², A. Roy¹⁶³, S. Roy-Garand¹⁵⁶, A. Rozanov¹⁰³, Z. M. A. Rozario⁵⁹, Y. Rozen¹⁵¹, A. Rubio Jimenez¹⁶⁴, A. J. Ruby⁹³, V. H. Ruelas Rivera¹⁸, T. A. Ruggeri¹, A. Ruggiero¹²⁷, A. Ruiz-Martinez¹⁶⁴, A. Rummler³⁶, Z. Rurikova⁵⁴, N. A. Rusakovich³⁸, H. L. Russell¹⁶⁶, G. Russo^{75a,75b}, J. P. Rutherford⁷, S. Rutherford Colmenares³², K. Rybacki⁹², M. Rybar¹³⁴, E. B. Rye¹²⁶, A. Ryzhov⁴⁴, J. A. Sabater Iglesias⁵⁶, P. Sabatini¹⁶⁴, H. F.-W. Sadrozinski¹³⁷, F. Safai Tehrani^{75a}, B. Safarzadeh Samani¹³⁵, S. Saha¹, M. Sahinsoy¹¹¹, A. Saibel¹⁶⁴, M. Saimpert¹³⁶, M. Saito¹⁵⁴, T. Saito¹⁵⁴, A. Sala^{71a,71b}, D. Salamani³⁶, A. Salmikov¹⁴⁴, J. Salt¹⁶⁴, A. Salvador Salas¹⁵², D. Salvatore^{43b,43a}, F. Salvatore¹⁴⁷, A. Salzburger³⁶, D. Sammel⁵⁴, E. Sampson⁹², D. Sampsonidis^{153,z}, D. Sampsonidou¹²⁴, J. Sánchez¹⁶⁴, V. Sanchez Sebastian¹⁶⁴, H. Sandaker¹²⁶, C. O. Sander⁴⁸, J. A. Sandesara¹⁰⁴, M. Sandhoff¹⁷², C. Sandoval^{22b}, D. P. C. Sankey¹³⁵, T. Sano⁸⁸, A. Sansoni⁵³, L. Santi^{75a,75b}, C. Santoni⁴⁰, H. Santos^{131a,131b}, A. Santra¹⁷⁰, K. A. Saoucha¹⁶¹, J. G. Saraiva^{131a,131d}, J. Sardain⁷, O. Sasaki⁸⁴, K. Sato¹⁵⁸, C. Sauer^{63b}, F. Sauerburger⁵⁴, E. Sauvan⁴, P. Savard^{156,e}, R. Sawada¹⁵⁴, C. Sawyer¹³⁵, L. Sawyer⁹⁸, I. Sayago Galvan¹⁶⁴, C. Sbarra^{23b}, A. Sbrizzi^{23b,23a}, T. Scanlon⁹⁷, J. Schaarschmidt¹³⁹, U. Schäfer¹⁰¹, A. C. Schaffer^{66,44}, D. Schaile¹¹⁰, R. D. Schamberger¹⁴⁶, C. Scharf¹⁸, M. M. Schefer¹⁹, V. A. Schegelsky³⁷, D. Scheirich¹³⁴, F. Schenck¹⁸, M. Schernau¹⁶⁰, C. Scheulen⁵⁵, C. Schiavi^{57b,57a}, M. Schioppa^{43b,43a}, B. Schlag^{144,s}, K. E. Schleicher⁵⁴, S. Schlenker³⁶, J. Schmeing¹⁷², M. A. Schmidt¹⁷², K. Schmieden¹⁰¹, C. Schmitt¹⁰¹, N. Schmitt¹⁰¹, S. Schmitt⁴⁸, L. Schoeffel¹³⁶, A. Schoening^{63b}, P. G. Scholer³⁴, E. Schopf¹²⁷, M. Schott¹⁰¹, J. Schovancova³⁶, S. Schramm⁵⁶, T. Schroer⁵⁶, H.-C. Schultz-Coulon^{63a}, M. Schumacher⁵⁴, B. A. Schumm¹³⁷, Ph. Schune¹³⁶, A. J. Schuy¹³⁹, H. R. Schwartz¹³⁷, A. Schwartzman¹⁴⁴, T. A. Schwarz¹⁰⁷, Ph. Schwemling¹³⁶, R. Schwienhorst¹⁰⁸, A. Sciandra²⁹, G. Sciolla²⁶, F. Scuri^{74a}, C. D. Sebastiani⁹³, K. Sedlaczek¹¹⁶, P. Seema¹⁸, S. C. Seidel¹¹³, A. Seiden¹³⁷, B. D. Seidlitz⁴¹, C. Seitz⁴⁸, J. M. Seixas^{83b}

G. Sekhniaidze^{72a} L. Selem⁶⁰ N. Semprini-Cesari^{23b,23a} D. Sengupta⁵⁶ V. Senthilkumar¹⁶⁴ L. Serin⁶⁶
L. Serkin^{69a,69b} M. Sessa^{76a,76b} H. Severini¹²¹ F. Sforza^{57b,57a} A. Sfyrila⁵⁶ Q. Sha^{14a} E. Shabalina⁵⁵
A. H. Shah³² R. Shaheen¹⁴⁵ J. D. Shahinian¹²⁹ D. Shaked Renous¹⁷⁰ L. Y. Shan^{14a} M. Shapiro^{17a}
A. Sharma³⁶ A. S. Sharma¹⁶⁵ P. Sharma⁸⁰ P. B. Shatalov³⁷ K. Shaw¹⁴⁷ S. M. Shaw¹⁰² A. Shcherbakova³⁷
Q. Shen^{62c,5} D. J. Sheppard¹⁴³ P. Sherwood⁹⁷ L. Shi⁹⁷ X. Shi^{14a} C. O. Shimmin¹⁷³ J. D. Shinner⁹⁶
I. P. J. Shipsey¹²⁷ S. Shirabe⁸⁹ M. Shiyakova^{38,gg} J. Shlomi¹⁷⁰ M. J. Shochet³⁹ J. Shojaii¹⁰⁶ D. R. Shope¹²⁶
B. Shrestha¹²¹ S. Shrestha^{120,hh} E. M. Shrif^{33g} M. J. Shroff¹⁶⁶ P. Sicho¹³² A. M. Sickles¹⁶³
E. Sideras Haddad^{33g} A. C. Sidley¹¹⁵ A. Sidoti^{23b} F. Siegert⁵⁰ Dj. Sijacki¹⁵ F. Sili⁹¹ J. M. Silva⁵²
M. V. Silva Oliveira²⁹ S. B. Silverstein^{47a} S. Simion⁶⁶ R. Simoniello³⁶ E. L. Simpson¹⁰² H. Simpson¹⁴⁷
L. R. Simpson¹⁰⁷ N. D. Simpson⁹⁹ S. Simsek⁸² S. Sindhu⁵⁵ P. Sinervo¹⁵⁶ S. Singh¹⁵⁶ S. Sinha⁴⁸ S. Sinha¹⁰²
M. Sioli^{23b,23a} I. Siral³⁶ E. Sitnikova⁴⁸ J. Sjölin^{47a,47b} A. Skaf⁵⁵ E. Skorda²⁰ P. Skubic¹²¹ M. Slawinska⁸⁷
V. Smakhtin¹⁷⁰ B. H. Smart¹³⁵ S. Yu. Smirnov³⁷ Y. Smirnov³⁷ L. N. Smirnova^{37,k} O. Smirnova⁹⁹
A. C. Smith⁴¹ D. R. Smith¹⁶⁰ E. A. Smith³⁹ H. A. Smith¹²⁷ J. L. Smith¹⁰² R. Smith¹⁴⁴ M. Smizanska⁹²
K. Smolek¹³³ A. A. Snesarev³⁷ S. R. Snider¹⁵⁶ H. L. Snoek¹¹⁵ S. Snyder²⁹ R. Sobie^{166,n} A. Soffer¹⁵²
C. A. Solans Sanchez³⁶ E. Yu. Soldatov³⁷ U. Soldevila¹⁶⁴ A. A. Solodkov³⁷ S. Solomon²⁶ A. Soloshenko³⁸
K. Solovieva⁵⁴ O. V. Solovyanov⁴⁰ V. Solovyev³⁷ P. Sommer³⁶ A. Sonay¹³ W. Y. Song^{157b} A. Sopczak¹³³
A. L. Sopio⁹⁷ F. Sopkova^{28b} J. D. Sorenson¹¹³ I. R. Sotarriva Alvarez¹⁵⁵ V. Sothilingam^{63a}
O. J. Soto Sandoval^{138c,138b} S. Sottocornola⁶⁸ R. Soualah¹⁶¹ Z. Soumami^{35e} D. South⁴⁸ N. Soybelman¹⁷⁰
S. Spagnolo^{70a,70b} M. Spalla¹¹¹ D. Sperlich⁵⁴ G. Spigo³⁶ S. Spinali⁹² D. P. Spiteri⁵⁹ M. Spousta¹³⁴
E. J. Staats³⁴ R. Stamen^{63a} A. Stampeki²⁰ M. Standke²⁴ E. Stanecka⁸⁷ W. Stanek-Maslouska⁴⁸
M. V. Stange⁵⁰ B. Stanislaus^{17a} M. M. Stanitzki⁴⁸ B. Stapf⁴⁸ E. A. Starchenko³⁷ G. H. Stark¹³⁷ J. Stark⁹⁰
P. Staroba¹³² P. Starovoitov^{63a} S. Stärz¹⁰⁵ R. Staszewski⁸⁷ G. Stavropoulos⁴⁶ J. Steentoft¹⁶² P. Steinberg²⁹
B. Stelzer^{143,157a} H. J. Stelzer¹³⁰ O. Stelzer-Chilton^{157a} H. Stenzel⁵⁸ T. J. Stevenson¹⁴⁷ G. A. Stewart³⁶
J. R. Stewart¹²² M. C. Stockton³⁶ G. Stoica^{27b} M. Stolarski^{131a} S. Stonjek¹¹¹ A. Straessner⁵⁰
J. Strandberg¹⁴⁵ S. Strandberg^{47a,47b} M. Stratmann¹⁷² M. Strauss¹²¹ T. Strebler¹⁰³ P. Strizenec^{28b}
R. Ströhmer¹⁶⁷ D. M. Strom¹²⁴ R. Stroynowski⁴⁴ A. Strubig^{47a,47b} S. A. Stucci²⁹ B. Stugu¹⁶ J. Stupak¹²¹
N. A. Styles⁴⁸ D. Su¹⁴⁴ S. Su^{62a} W. Su^{62d} X. Su^{62a} D. Suchy^{28a} K. Sugizaki¹⁵⁴ V. V. Sulim³⁷
M. J. Sullivan⁹³ D. M. S. Sultan¹²⁷ L. Sultanaliev³⁷ S. Sultansoy^{3b} T. Sumida⁸⁸ S. Sun¹⁰⁷ S. Sun¹⁷¹
O. Sunneborn Gudnadottir¹⁶² N. Sur¹⁰³ M. R. Sutton¹⁴⁷ H. Suzuki¹⁵⁸ M. Svatos¹³² M. Swiatlowski^{157a}
T. Swirski¹⁶⁷ I. Sykora^{28a} M. Sykora¹³⁴ T. Sykora¹³⁴ D. Ta¹⁰¹ K. Tackmann^{48,ff} A. Taffard¹⁶⁰
R. Tahirout^{157a} J. S. Tafoya Vargas⁶⁶ Y. Takubo⁸⁴ M. Talby¹⁰³ A. A. Talyshev³⁷ K. C. Tam^{64b} N. M. Tamir¹⁵²
A. Tanaka¹⁵⁴ J. Tanaka¹⁵⁴ R. Tanaka⁶⁶ M. Tanasini^{57b,57a} Z. Tao¹⁶⁵ S. Tapia Araya^{138f} S. Tapprogge¹⁰¹
A. Tarek Abouelfadl Mohamed¹⁰⁸ S. Tarem¹⁵¹ K. Tariq^{14a} G. Tarna^{27b} G. F. Tartarelli^{71a} M. J. Tartarin⁹⁰
P. Tas¹³⁴ M. Tasevsky¹³² E. Tassi^{43b,43a} A. C. Tate¹⁶³ G. Tateno¹⁵⁴ Y. Tayalati^{35c,ii} G. N. Taylor¹⁰⁶
W. Taylor^{157b} A. S. Tee¹⁷¹ R. Teixeira De Lima¹⁴⁴ P. Teixeira-Dias⁹⁶ J. J. Teoh¹⁵⁶ K. Terashi¹⁵⁴ J. Terron¹⁰⁰
S. Terzo¹³ M. Testa⁵³ R. J. Teuscher^{156,n} A. Thaler⁷⁹ O. Theiner⁵⁶ N. Themistokleous⁵²
T. Thevenaux-Pelzer¹⁰³ O. Thielmann¹⁷² D. W. Thomas⁹⁶ J. P. Thomas²⁰ E. A. Thompson^{17a}
P. D. Thompson²⁰ E. Thomson¹²⁹ R. E. Thornberry⁴⁴ Y. Tian⁵⁵ V. Tikhomirov^{37,k} Yu. A. Tikhonov³⁷
S. Timoshenko³⁷ D. Timoshyn¹³⁴ E. X. L. Ting¹ P. Tipton¹⁷³ S. H. Tlou^{33g} K. Todome¹⁵⁵
S. Todorova-Nova¹³⁴ S. Todt⁵⁰ M. Togawa⁸⁴ J. Tojo⁸⁹ S. Tokár^{28a} K. Tokushuku⁸⁴ O. Toldaiev⁶⁸
R. Tombs³² M. Tomoto^{84,112} L. Tompkins^{144,s} K. W. Topolnicki^{86b} E. Torrence¹²⁴ H. Torres⁹⁰
E. Torró Pastor¹⁶⁴ M. Toscani³⁰ C. Toscirri³⁹ M. Tost¹¹ D. R. Tovey¹⁴⁰ A. Traeet¹⁶ I. S. Trandafir^{27b}
T. Trefzger¹⁶⁷ A. Tricoli²⁹ I. M. Trigger^{157a} S. Trincaz-Duvoid¹²⁸ D. A. Trischuk²⁶ B. Trocmé⁶⁰
L. Truong^{33c} M. Trzebinski⁸⁷ A. Trzupek⁸⁷ F. Tsai¹⁴⁶ M. Tsai¹⁰⁷ A. Tsiamis^{153,z} P. V. Tsiarehka³⁷
S. Tsigaridas^{157a} A. Tsigotidis^{153,aa} V. Tsiskaridze¹⁵⁶ E. G. Tskhadadze^{150a} M. Tsopoulou¹⁵³ Y. Tsujikawa⁸⁸
I. I. Tsukerman³⁷ V. Tsulaia^{17a} S. Tsuno⁸⁴ K. Tsurii¹¹⁹ D. Tsybychev¹⁴⁶ Y. Tu^{64b} A. Tudorache^{27b}
V. Tudorache^{27b} A. N. Tuna⁶¹ S. Turchikhin^{57b,57a} I. Turk Cakir^{3a} R. Turra^{71a} T. Turtuvshin^{38,ij} P. M. Tuts⁴¹
S. Tzamarias^{153,z} E. Tzovara¹⁰¹ F. Ukegawa¹⁵⁸ P. A. Ulloa Poblete^{138c,138b} E. N. Umaka²⁹ G. Unal³⁶
A. Undrus²⁹ G. Unel¹⁶⁰ J. Urban^{28b} P. Urquijo¹⁰⁶ P. Urrejola^{138a} G. Usai⁸ R. Ushioda¹⁵⁵ M. Usman¹⁰⁹

Z. Uysal⁸² V. Vacek¹³³ B. Vachon¹⁰⁵ K. O. H. Vadla¹²⁶ T. Vafeiadis³⁶ A. Vaitkus⁹⁷ C. Valderanis¹¹⁰
E. Valdes Santurio^{47a,47b} M. Valente^{157a} S. Valentinetti^{23b,23a} A. Valero¹⁶⁴ E. Valiente Moreno¹⁶⁴ A. Vallier⁹⁰
J. A. Valls Ferrer¹⁶⁴ D. R. Van Arneman¹¹⁵ T. R. Van Daalen¹³⁹ A. Van Der Graaf⁴⁹ P. Van Gemmeren⁶
M. Van Rijnbach¹²⁶ S. Van Stroud⁹⁷ I. Van Vulpen¹¹⁵ P. Vana¹³⁴ M. Vanadia^{76a,76b} W. Vandelli³⁶
E. R. Vandewall¹²² D. Vannicola¹⁵² L. Vannoli⁵³ R. Vari^{75a} E. W. Varnes⁷ C. Varni^{17b} T. Varol¹⁴⁹
D. Varouchas⁶⁶ L. Varriale¹⁶⁴ K. E. Varvell¹⁴⁸ M. E. Vasile^{27b} L. Vaslin⁸⁴ G. A. Vasquez¹⁶⁶ A. Vasyukov³⁸
R. Vavricka¹⁰¹ F. Vazeille⁴⁰ T. Vazquez Schroeder³⁶ J. Veatch³¹ V. Vecchio¹⁰² M. J. Veen¹⁰⁴ I. Veliscek²⁹
L. M. Veloce¹⁵⁶ F. Veloso^{131a,131c} S. Veneziano^{75a} A. Ventura^{70a,70b} S. Ventura Gonzalez¹³⁶ A. Verbytskyi¹¹¹
M. Verducci^{74a,74b} C. Vergis⁹⁵ M. Verissimo De Araujo^{83b} W. Verkerke¹¹⁵ J. C. Vermeulen¹¹⁵ C. Vernieri¹⁴⁴
M. Vessella¹⁰⁴ M. C. Vetterli^{143,e} A. Vgenopoulos^{153,z} N. Viaux Maira^{138f} T. Vickey¹⁴⁰ O. E. Vickey Boeriu¹⁴⁰
G. H. A. Viehhauser¹²⁷ L. Vigani^{63b} M. Villa^{23b,23a} M. Villaplana Perez¹⁶⁴ E. M. Villhauer⁵² E. Vilucchi⁵³
M. G. Vinciter³⁴ G. S. Virdee²⁰ A. Vishwakarma⁵² A. Visibile¹¹⁵ C. Vittori³⁶ I. Vivarelli^{23b,23a} E. Voevodina¹¹¹
F. Vogel¹¹⁰ J. C. Voigt⁵⁰ P. Vokac¹³³ Yu. Volkotrub^{86b} J. Von Ahnen⁴⁸ E. Von Toerne²⁴ B. Vormwald³⁶
V. Vorobel¹³⁴ K. Vorobev³⁷ M. Vos¹⁶⁴ K. Voss¹⁴² M. Vozak¹¹⁵ L. Vozdecky¹²¹ N. Vranjes¹⁵
M. Vranjes Milosavljevic¹⁵ M. Vreeswijk¹¹⁵ N. K. Vu^{62d,62c} R. Vuillermet³⁶ O. Vujanovic¹⁰¹ I. Vukotic³⁹
S. Wada¹⁵⁸ C. Wagner¹⁰⁴ J. M. Wagner^{17a} W. Wagner¹⁷² S. Wahdan¹⁷² H. Wahlberg⁹¹ M. Wakida¹¹²
J. Walder¹³⁵ R. Walker¹¹⁰ W. Walkowiak¹⁴² A. Wall¹²⁹ E. J. Wallin⁹⁹ T. Wamorkar⁶ A. Z. Wang¹³⁷
C. Wang¹⁰¹ C. Wang¹¹ H. Wang^{17a} J. Wang^{64c} R.-J. Wang¹⁰¹ R. Wang⁶¹ R. Wang⁶ S. M. Wang¹⁴⁹
S. Wang^{62b} T. Wang^{62a} W. T. Wang⁸⁰ W. Wang^{14a} X. Wang^{14c} X. Wang¹⁶³ X. Wang^{62c} Y. Wang^{62d}
Y. Wang^{14c} Z. Wang¹⁰⁷ Z. Wang^{62d,51,62c} Z. Wang¹⁰⁷ A. Warburton¹⁰⁵ R. J. Ward²⁰ N. Warrack⁵⁹
S. Waterhouse⁹⁶ A. T. Watson²⁰ H. Watson⁵⁹ M. F. Watson²⁰ E. Watton^{59,135} G. Watts¹³⁹ B. M. Waugh⁹⁷
J. M. Webb⁵⁴ C. Weber²⁹ H. A. Weber¹⁸ M. S. Weber¹⁹ S. M. Weber^{63a} C. Wei^{62a} Y. Wei¹²⁷
A. R. Weidberg¹²⁷ E. J. Weik¹¹⁸ J. Weingarten⁴⁹ M. Weirich¹⁰¹ C. Weiser⁵⁴ C. J. Wells⁴⁸ T. Wenaus²⁹
B. Wendland⁴⁹ T. Wengler³⁶ N. S. Wenke¹¹¹ N. Wermes²⁴ M. Wessels^{63a} A. M. Wharton⁹² A. S. White⁶¹
A. White⁸ M. J. White¹ D. Whiteson¹⁶⁰ L. Wickremasinghe¹²⁵ W. Wiedenmann¹⁷¹ M. Wielers¹³⁵
C. Wiglesworth⁴² D. J. Wilbern¹²¹ H. G. Wilkens³⁶ J. J. H. Wilkinson³² D. M. Williams⁴¹ H. H. Williams¹²⁹
S. Williams³² S. Willocq¹⁰⁴ B. J. Wilson¹⁰² P. J. Windischhofer³⁹ F. I. Winkel³⁰ F. Winklmeier¹²⁴
B. T. Winter⁵⁴ J. K. Winter¹⁰² M. Wittgen¹⁴⁴ M. Wobisch⁹⁸ Z. Wolffs¹¹⁵ J. Wollrath¹⁶⁰ M. W. Wolter⁸⁷
H. Wolters^{131a,131c} M. C. Wong¹³⁷ E. L. Woodward⁴¹ S. D. Worm⁴⁸ B. K. Wosiek⁸⁷ K. W. Woźniak⁸⁷
S. Wozniowski⁵⁵ K. Wraight⁵⁹ C. Wu²⁰ M. Wu^{14d} M. Wu¹¹⁴ S. L. Wu¹⁷¹ X. Wu⁵⁶ Y. Wu^{62a} Z. Wu⁴
J. Wuerzinger^{111,v} T. R. Wyatt¹⁰² B. M. Wynne⁵² S. Xella⁴² L. Xia^{14c} M. Xia^{14b} J. Xiang^{64c} M. Xie^{62a}
X. Xie^{62a} S. Xin^{14a,14e} A. Xiong¹²⁴ J. Xiong^{17a} D. Xu^{14a} H. Xu^{62a} L. Xu^{62a} R. Xu¹²⁹ T. Xu¹⁰⁷ Y. Xu^{14b}
Z. Xu⁵² Z. Xu^{14c} B. Yabsley¹⁴⁸ S. Yacoob^{33a} Y. Yamaguchi¹⁵⁵ E. Yamashita¹⁵⁴ H. Yamauchi¹⁵⁸
T. Yamazaki^{17a} Y. Yamazaki⁸⁵ J. Yan^{62c} S. Yan⁵⁹ Z. Yan¹⁰⁴ H. J. Yang^{62c,62d} H. T. Yang^{62a} S. Yang^{62a}
T. Yang^{64c} X. Yang³⁶ X. Yang^{14a} Y. Yang⁴⁴ Y. Yang^{62a} Z. Yang^{62a} W.-M. Yao^{17a} H. Ye^{14c} H. Ye⁵⁵
J. Ye^{14a} S. Ye²⁹ X. Ye^{62a} Y. Yeh⁹⁷ I. Yeletsikh³⁸ B. K. Yeo^{17b} M. R. Yexley⁹⁷ P. Yin⁴¹ K. Yorita¹⁶⁹
S. Younas^{27b} C. J. S. Young³⁶ C. Young¹⁴⁴ C. Yu^{14a,14e} Y. Yu^{62a} M. Yuan¹⁰⁷ R. Yuan^{62d} L. Yue⁹⁷
M. Zaazoua^{62a} B. Zabinski⁸⁷ E. Zaid⁵² Z. K. Zak⁸⁷ T. Zakareishvili¹⁶⁴ N. Zakharchuk³⁴ S. Zambito⁵⁶
J. A. Zamora Saa^{138d,138b} J. Zang¹⁵⁴ D. Zanzi⁵⁴ O. Zaplatilek¹³³ C. Zeitnitz¹⁷² H. Zeng^{14a} J. C. Zeng¹⁶³
D. T. Zenger Jr.²⁶ O. Zenin³⁷ T. Ženiš^{28a} S. Zenz⁹⁵ S. Zerradi^{35a} D. Zerwas⁶⁶ M. Zhai^{14a,14e} D. F. Zhang¹⁴⁰
J. Zhang^{62b} J. Zhang⁶ K. Zhang^{14a,14e} L. Zhang^{62a} L. Zhang^{14c} P. Zhang^{14a,14e} R. Zhang¹⁷¹ S. Zhang¹⁰⁷
S. Zhang⁴⁴ T. Zhang¹⁵⁴ X. Zhang^{62c} X. Zhang^{62b} Y. Zhang^{62c,5} Y. Zhang⁹⁷ Y. Zhang^{14c} Z. Zhang^{17a}
Z. Zhang⁶⁶ H. Zhao¹³⁹ T. Zhao^{62b} Y. Zhao¹³⁷ Z. Zhao^{62a} Z. Zhao^{62a} A. Zhemchugov³⁸ J. Zheng^{14c}
K. Zheng¹⁶³ X. Zheng^{62a} Z. Zheng¹⁴⁴ D. Zhong¹⁶³ B. Zhou¹⁰⁷ H. Zhou⁷ N. Zhou^{62c} Y. Zhou^{14c} Y. Zhou,
C. G. Zhu^{62b} J. Zhu¹⁰⁷ Y. Zhu^{62c} Y. Zhu^{62a} X. Zhuang^{14a} K. Zhukov³⁷ N. I. Zimine³⁸ J. Zinsser^{63b}
M. Ziolkowski¹⁴² L. Živković¹⁵ A. Zoccoli^{23b,23a} K. Zoch⁶¹ T. G. Zorbas¹⁴⁰ O. Zormpa⁴⁶
W. Zou⁴¹ and L. Zwalinski³⁶

(ATLAS Collaboration)

- ¹*Department of Physics, University of Adelaide, Adelaide, Australia*
- ²*Department of Physics, University of Alberta, Edmonton Alberta, Canada*
- ^{3a}*Department of Physics, Ankara University, Ankara, Türkiye*
- ^{3b}*Division of Physics, TOBB University of Economics and Technology, Ankara, Türkiye*
- ⁴*LAPP, Université Savoie Mont Blanc, CNRS/IN2P3, Annecy, France*
- ⁵*APC, Université Paris Cité, CNRS/IN2P3, Paris, France*
- ⁶*High Energy Physics Division, Argonne National Laboratory, Argonne, Illinois, USA*
- ⁷*Department of Physics, University of Arizona, Tucson, Arizona, USA*
- ⁸*Department of Physics, University of Texas at Arlington, Arlington, Texas, USA*
- ⁹*Physics Department, National and Kapodistrian University of Athens, Athens, Greece*
- ¹⁰*Physics Department, National Technical University of Athens, Zografou, Greece*
- ¹¹*Department of Physics, University of Texas at Austin, Austin, Texas, USA*
- ¹²*Institute of Physics, Azerbaijan Academy of Sciences, Baku, Azerbaijan*
- ¹³*Institut de Física d'Altes Energies (IFAE), Barcelona Institute of Science and Technology, Barcelona, Spain*
- ^{14a}*Institute of High Energy Physics, Chinese Academy of Sciences, Beijing, China*
- ^{14b}*Physics Department, Tsinghua University, Beijing, China*
- ^{14c}*Department of Physics, Nanjing University, Nanjing, China*
- ^{14d}*School of Science, Shenzhen Campus of Sun Yat-sen University, China*
- ^{14e}*University of Chinese Academy of Science (UCAS), Beijing, China*
- ¹⁵*Institute of Physics, University of Belgrade, Belgrade, Serbia*
- ¹⁶*Department for Physics and Technology, University of Bergen, Bergen, Norway*
- ^{17a}*Physics Division, Lawrence Berkeley National Laboratory, Berkeley, California, USA*
- ^{17b}*University of California, Berkeley, California, USA*
- ¹⁸*Institut für Physik, Humboldt Universität zu Berlin, Berlin, Germany*
- ¹⁹*Albert Einstein Center for Fundamental Physics and Laboratory for High Energy Physics, University of Bern, Bern, Switzerland*
- ²⁰*School of Physics and Astronomy, University of Birmingham, Birmingham, United Kingdom*
- ^{21a}*Department of Physics, Bogazici University, Istanbul, Türkiye*
- ^{21b}*Department of Physics Engineering, Gaziantep University, Gaziantep, Türkiye*
- ^{21c}*Department of Physics, Istanbul University, Istanbul, Türkiye*
- ^{22a}*Facultad de Ciencias y Centro de Investigaciones, Universidad Antonio Nariño, Bogotá, Colombia*
- ^{22b}*Departamento de Física, Universidad Nacional de Colombia, Bogotá, Colombia*
- ^{23a}*Dipartimento di Fisica e Astronomia A. Righi, Università di Bologna, Bologna, Italy*
- ^{23b}*INFN Sezione di Bologna, Italy*
- ²⁴*Physikalisches Institut, Universität Bonn, Bonn, Germany*
- ²⁵*Department of Physics, Boston University, Boston, Massachusetts, USA*
- ²⁶*Department of Physics, Brandeis University, Waltham, Massachusetts, USA*
- ^{27a}*Transilvania University of Brasov, Brasov, Romania*
- ^{27b}*Horia Hulubei National Institute of Physics and Nuclear Engineering, Bucharest, Romania*
- ^{27c}*Department of Physics, Alexandru Ioan Cuza University of Iasi, Iasi, Romania*
- ^{27d}*National Institute for Research and Development of Isotopic and Molecular Technologies, Physics Department, Cluj-Napoca, Romania*
- ^{27e}*National University of Science and Technology Politehnica, Bucharest, Romania*
- ^{27f}*West University in Timisoara, Timisoara, Romania*
- ^{27g}*Faculty of Physics, University of Bucharest, Bucharest, Romania*
- ^{28a}*Faculty of Mathematics, Physics and Informatics, Comenius University, Bratislava, Slovak Republic*
- ^{28b}*Department of Subnuclear Physics, Institute of Experimental Physics of the Slovak Academy of Sciences, Kosice, Slovak Republic*
- ²⁹*Physics Department, Brookhaven National Laboratory, Upton, New York, USA*
- ³⁰*Universidad de Buenos Aires, Facultad de Ciencias Exactas y Naturales, Departamento de Física, y CONICET, Instituto de Física de Buenos Aires (IFIBA), Buenos Aires, Argentina*
- ³¹*California State University, California, USA*
- ³²*Cavendish Laboratory, University of Cambridge, Cambridge, United Kingdom*
- ^{33a}*Department of Physics, University of Cape Town, Cape Town, South Africa*
- ^{33b}*iThemba Labs, Western Cape, South Africa*
- ^{33c}*Department of Mechanical Engineering Science, University of Johannesburg, Johannesburg, South Africa*
- ^{33d}*National Institute of Physics, University of the Philippines Diliman (Philippines), Philippines*
- ^{33e}*University of South Africa, Department of Physics, Pretoria, South Africa*
- ^{33f}*University of Zululand, KwaDlangezwa, South Africa*

- ^{33g}*School of Physics, University of the Witwatersrand, Johannesburg, South Africa*
- ³⁴*Department of Physics, Carleton University, Ottawa, Ontario, Canada*
- ^{35a}*Faculté des Sciences Ain Chock, Réseau Universitaire de Physique des Hautes Energies—Université Hassan II, Casablanca, Morocco*
- ^{35b}*Faculté des Sciences, Université Ibn-Tofail, Kénitra, Morocco*
- ^{35c}*Faculté des Sciences Semlalia, Université Cadi Ayyad, LPHEA-Marrakech, Morocco*
- ^{35d}*LPMR, Faculté des Sciences, Université Mohamed Premier, Oujda, Morocco*
- ^{35e}*Faculté des sciences, Université Mohammed V, Rabat, Morocco*
- ^{35f}*Institute of Applied Physics, Mohammed VI Polytechnic University, Ben Guerir, Morocco*
- ³⁶*CERN, Geneva, Switzerland*
- ³⁷*Affiliated with an institute covered by a cooperation agreement with CERN*
- ³⁸*Affiliated with an international laboratory covered by a cooperation agreement with CERN*
- ³⁹*Enrico Fermi Institute, University of Chicago, Chicago, Illinois, USA*
- ⁴⁰*LPC, Université Clermont Auvergne, CNRS/IN2P3, Clermont-Ferrand, France*
- ⁴¹*Nevis Laboratory, Columbia University, Irvington, New York, USA*
- ⁴²*Niels Bohr Institute, University of Copenhagen, Copenhagen, Denmark*
- ^{43a}*Dipartimento di Fisica, Università della Calabria, Rende, Italy*
- ^{43b}*INFN Gruppo Collegato di Cosenza, Laboratori Nazionali di Frascati, Italy*
- ⁴⁴*Physics Department, Southern Methodist University, Dallas, Texas, USA*
- ⁴⁵*Physics Department, University of Texas at Dallas, Richardson, Texas, USA*
- ⁴⁶*National Centre for Scientific Research “Demokritos”, Agia Paraskevi, Greece*
- ^{47a}*Department of Physics, Stockholm University, Sweden*
- ^{47b}*Oskar Klein Centre, Stockholm, Sweden*
- ⁴⁸*Deutsches Elektronen-Synchrotron DESY, Hamburg and Zeuthen, Germany*
- ⁴⁹*Fakultät Physik, Technische Universität Dortmund, Dortmund, Germany*
- ⁵⁰*Institut für Kern- und Teilchenphysik, Technische Universität Dresden, Dresden, Germany*
- ⁵¹*Department of Physics, Duke University, Durham, North Carolina, USA*
- ⁵²*SUPA - School of Physics and Astronomy, University of Edinburgh, Edinburgh, United Kingdom*
- ⁵³*INFN e Laboratori Nazionali di Frascati, Frascati, Italy*
- ⁵⁴*Physikalisches Institut, Albert-Ludwigs-Universität Freiburg, Freiburg, Germany*
- ⁵⁵*II. Physikalisches Institut, Georg-August-Universität Göttingen, Göttingen, Germany*
- ⁵⁶*Département de Physique Nucléaire et Corpusculaire, Université de Genève, Genève, Switzerland*
- ^{57a}*Dipartimento di Fisica, Università di Genova, Genova, Italy*
- ^{57b}*INFN Sezione di Genova, Italy*
- ⁵⁸*II. Physikalisches Institut, Justus-Liebig-Universität Giessen, Giessen, Germany*
- ⁵⁹*SUPA - School of Physics and Astronomy, University of Glasgow, Glasgow, United Kingdom*
- ⁶⁰*LPSC, Université Grenoble Alpes, CNRS/IN2P3, Grenoble INP, Grenoble, France*
- ⁶¹*Laboratory for Particle Physics and Cosmology, Harvard University, Cambridge, Massachusetts, USA*
- ^{62a}*Department of Modern Physics and State Key Laboratory of Particle Detection and Electronics, University of Science and Technology of China, Hefei, China*
- ^{62b}*Institute of Frontier and Interdisciplinary Science and Key Laboratory of Particle Physics and Particle Irradiation (MOE), Shandong University, Qingdao, China*
- ^{62c}*School of Physics and Astronomy, Shanghai Jiao Tong University, Key Laboratory for Particle Astrophysics and Cosmology (MOE), SKLPPC, Shanghai, China*
- ^{62d}*Tsung-Dao Lee Institute, Shanghai, China*
- ^{62e}*School of Physics and Microelectronics, Zhengzhou University, China*
- ^{63a}*Kirchhoff-Institut für Physik, Ruprecht-Karls-Universität Heidelberg, Heidelberg, Germany*
- ^{63b}*Physikalisches Institut, Ruprecht-Karls-Universität Heidelberg, Heidelberg, Germany*
- ^{64a}*Department of Physics, Chinese University of Hong Kong, Shatin, N.T., Hong Kong, China*
- ^{64b}*Department of Physics, University of Hong Kong, Hong Kong, China*
- ^{64c}*Department of Physics and Institute for Advanced Study, Hong Kong University of Science and Technology, Clear Water Bay, Kowloon, Hong Kong, China*
- ⁶⁵*Department of Physics, National Tsing Hua University, Hsinchu, Taiwan*
- ⁶⁶*IJCLab, Université Paris-Saclay, CNRS/IN2P3, 91405, Orsay, France*
- ⁶⁷*Centro Nacional de Microelectrónica (IMB-CNM-CSIC), Barcelona, Spain*
- ⁶⁸*Department of Physics, Indiana University, Bloomington, Indiana, USA*
- ^{69a}*INFN Gruppo Collegato di Udine, Sezione di Trieste, Udine, Italy*
- ^{69b}*ICTP, Trieste, Italy*
- ^{69c}*Dipartimento Politecnico di Ingegneria e Architettura, Università di Udine, Udine, Italy*
- ^{70a}*INFN Sezione di Lecce, Italy*

- ^{70b}*Dipartimento di Matematica e Fisica, Università del Salento, Lecce, Italy*
^{71a}*INFN Sezione di Milano, Italy*
- ^{71b}*Dipartimento di Fisica, Università di Milano, Milano, Italy*
^{72a}*INFN Sezione di Napoli, Italy*
- ^{72b}*Dipartimento di Fisica, Università di Napoli, Napoli, Italy*
^{73a}*INFN Sezione di Pavia, Italy*
- ^{73b}*Dipartimento di Fisica, Università di Pavia, Pavia, Italy*
^{74a}*INFN Sezione di Pisa, Italy*
- ^{74b}*Dipartimento di Fisica E. Fermi, Università di Pisa, Pisa, Italy*
^{75a}*INFN Sezione di Roma, Italy*
- ^{75b}*Dipartimento di Fisica, Sapienza Università di Roma, Roma, Italy*
^{76a}*INFN Sezione di Roma Tor Vergata, Italy*
- ^{76b}*Dipartimento di Fisica, Università di Roma Tor Vergata, Roma, Italy*
^{77a}*INFN Sezione di Roma Tre, Italy*
- ^{77b}*Dipartimento di Matematica e Fisica, Università Roma Tre, Roma, Italy*
^{78a}*INFN-TIFPA, Italy*
^{78b}*Università degli Studi di Trento, Trento, Italy*
- ⁷⁹*Universität Innsbruck, Department of Astro and Particle Physics, Innsbruck, Austria*
⁸⁰*University of Iowa, Iowa City IA, USA*
- ⁸¹*Department of Physics and Astronomy, Iowa State University, Ames, Iowa, USA*
⁸²*Istinye University, Sariyer, Istanbul, Türkiye*
- ^{83a}*Departamento de Engenharia Elétrica, Universidade Federal de Juiz de Fora (UFJF), Juiz de Fora, Brazil*
^{83b}*Universidade Federal do Rio De Janeiro COPPE/EE/IF, Rio de Janeiro, Brazil*
^{83c}*Instituto de Física, Universidade de São Paulo, São Paulo, Brazil*
^{83d}*Rio de Janeiro State University, Rio de Janeiro, Brazil*
^{83e}*Federal University of Bahia, Bahia, Brazil*
- ⁸⁴*KEK, High Energy Accelerator Research Organization, Tsukuba, Japan*
⁸⁵*Graduate School of Science, Kobe University, Kobe, Japan*
- ^{86a}*AGH University of Krakow, Faculty of Physics and Applied Computer Science, Krakow, Poland*
^{86b}*Marian Smoluchowski Institute of Physics, Jagiellonian University, Krakow, Poland*
- ⁸⁷*Institute of Nuclear Physics Polish Academy of Sciences, Krakow, Poland*
⁸⁸*Faculty of Science, Kyoto University, Kyoto, Japan*
- ⁸⁹*Research Center for Advanced Particle Physics and Department of Physics, Kyushu University, Fukuoka, Japan*
⁹⁰*L2IT, Université de Toulouse, CNRS/IN2P3, UPS, Toulouse, France*
- ⁹¹*Instituto de Física La Plata, Universidad Nacional de La Plata and CONICET, La Plata, Argentina*
⁹²*Physics Department, Lancaster University, Lancaster, United Kingdom*
⁹³*Oliver Lodge Laboratory, University of Liverpool, Liverpool, United Kingdom*
- ⁹⁴*Department of Experimental Particle Physics, Jožef Stefan Institute and Department of Physics, University of Ljubljana, Ljubljana, Slovenia*
⁹⁵*School of Physics and Astronomy, Queen Mary University of London, London, United Kingdom*
⁹⁶*Department of Physics, Royal Holloway University of London, Egham, United Kingdom*
⁹⁷*Department of Physics and Astronomy, University College London, London, United Kingdom*
⁹⁸*Louisiana Tech University, Ruston, Louisiana, USA*
⁹⁹*Fysiska institutionen, Lunds universitet, Lund, Sweden*
- ¹⁰⁰*Departamento de Física Teórica C-15 and CIAFF, Universidad Autónoma de Madrid, Madrid, Spain*
¹⁰¹*Institut für Physik, Universität Mainz, Mainz, Germany*
- ¹⁰²*School of Physics and Astronomy, University of Manchester, Manchester, United Kingdom*
¹⁰³*CPPM, Aix-Marseille Université, CNRS/IN2P3, Marseille, France*
- ¹⁰⁴*Department of Physics, University of Massachusetts, Amherst, Massachusetts, USA*
¹⁰⁵*Department of Physics, McGill University, Montreal, Quebec, Canada*
¹⁰⁶*School of Physics, University of Melbourne, Victoria, Australia*
- ¹⁰⁷*Department of Physics, University of Michigan, Ann Arbor, Michigan, USA*
- ¹⁰⁸*Department of Physics and Astronomy, Michigan State University, East Lansing, Michigan, USA*
¹⁰⁹*Group of Particle Physics, University of Montreal, Montreal, Quebec, Canada*
- ¹¹⁰*Fakultät für Physik, Ludwig-Maximilians-Universität München, München, Germany*
¹¹¹*Max-Planck-Institut für Physik (Werner-Heisenberg-Institut), München, Germany*
- ¹¹²*Graduate School of Science and Kobayashi-Maskawa Institute, Nagoya University, Nagoya, Japan*
¹¹³*Department of Physics and Astronomy, University of New Mexico, Albuquerque, New Mexico, USA*
- ¹¹⁴*Institute for Mathematics, Astrophysics and Particle Physics, Radboud University/Nikhef, Nijmegen, Netherlands*
¹¹⁵*Nikhef National Institute for Subatomic Physics and University of Amsterdam, Amsterdam, Netherlands*

- ¹¹⁶*Department of Physics, Northern Illinois University, DeKalb, Illinois, USA*
^{117a}*New York University Abu Dhabi, Abu Dhabi, United Arab Emirates*
^{117b}*United Arab Emirates University, Al Ain, United Arab Emirates*
¹¹⁸*Department of Physics, New York University, New York, New York, USA*
¹¹⁹*Ochanomizu University, Otsuka, Bunkyo-ku, Tokyo, Japan*
¹²⁰*Ohio State University, Columbus, Ohio, USA*
¹²¹*Homer L. Dodge Department of Physics and Astronomy, University of Oklahoma, Norman, Oklahoma, USA*
¹²²*Department of Physics, Oklahoma State University, Stillwater, Oklahoma, USA*
¹²³*Palacký University, Joint Laboratory of Optics, Olomouc, Czech Republic*
¹²⁴*Institute for Fundamental Science, University of Oregon, Eugene, Oregon, USA*
¹²⁵*Graduate School of Science, Osaka University, Osaka, Japan*
¹²⁶*Department of Physics, University of Oslo, Oslo, Norway*
¹²⁷*Department of Physics, Oxford University, Oxford, United Kingdom*
¹²⁸*LPNHE, Sorbonne Université, Université Paris Cité, CNRS/IN2P3, Paris, France*
¹²⁹*Department of Physics, University of Pennsylvania, Philadelphia, Pennsylvania, USA*
¹³⁰*Department of Physics and Astronomy, University of Pittsburgh, Pittsburgh, Pennsylvania, USA*
^{131a}*Laboratório de Instrumentação e Física Experimental de Partículas—LIP, Lisboa, Portugal*
^{131b}*Departamento de Física, Faculdade de Ciências, Universidade de Lisboa, Lisboa, Portugal*
^{131c}*Departamento de Física, Universidade de Coimbra, Coimbra, Portugal*
^{131d}*Centro de Física Nuclear da Universidade de Lisboa, Lisboa, Portugal*
^{131e}*Departamento de Física, Universidade do Minho, Braga, Portugal*
^{131f}*Departamento de Física Teórica y del Cosmos, Universidad de Granada, Granada (Spain), Spain*
^{131g}*Departamento de Física, Instituto Superior Técnico, Universidade de Lisboa, Lisboa, Portugal*
¹³²*Institute of Physics of the Czech Academy of Sciences, Prague, Czech Republic*
¹³³*Czech Technical University in Prague, Prague, Czech Republic*
¹³⁴*Charles University, Faculty of Mathematics and Physics, Prague, Czech Republic*
¹³⁵*Particle Physics Department, Rutherford Appleton Laboratory, Didcot, United Kingdom*
¹³⁶*IRFU, CEA, Université Paris-Saclay, Gif-sur-Yvette, France*
¹³⁷*Santa Cruz Institute for Particle Physics, University of California Santa Cruz, Santa Cruz, California, USA*
^{138a}*Departamento de Física, Pontificia Universidad Católica de Chile, Santiago, Chile*
^{138b}*Millennium Institute for Subatomic physics at high energy frontier (SAPHIR), Santiago, Chile*
^{138c}*Instituto de Investigación Multidisciplinario en Ciencia y Tecnología, y Departamento de Física, Universidad de La Serena, Chile*
^{138d}*Universidad Andres Bello, Department of Physics, Santiago, Chile*
^{138e}*Instituto de Alta Investigación, Universidad de Tarapacá, Arica, Chile*
^{138f}*Departamento de Física, Universidad Técnica Federico Santa María, Valparaíso, Chile*
¹³⁹*Department of Physics, University of Washington, Seattle, Washington, USA*
¹⁴⁰*Department of Physics and Astronomy, University of Sheffield, Sheffield, United Kingdom*
¹⁴¹*Department of Physics, Shinshu University, Nagano, Japan*
¹⁴²*Department Physik, Universität Siegen, Siegen, Germany*
¹⁴³*Department of Physics, Simon Fraser University, Burnaby, British Columbia, Canada*
¹⁴⁴*SLAC National Accelerator Laboratory, Stanford, California, USA*
¹⁴⁵*Department of Physics, Royal Institute of Technology, Stockholm, Sweden*
¹⁴⁶*Departments of Physics and Astronomy, Stony Brook University, Stony Brook, New York, USA*
¹⁴⁷*Department of Physics and Astronomy, University of Sussex, Brighton, United Kingdom*
¹⁴⁸*School of Physics, University of Sydney, Sydney, Australia*
¹⁴⁹*Institute of Physics, Academia Sinica, Taipei, Taiwan*
^{150a}*E. Andronikashvili Institute of Physics, Iv. Javakhishvili Tbilisi State University, Tbilisi, Georgia*
^{150b}*High Energy Physics Institute, Tbilisi State University, Tbilisi, Georgia*
^{150c}*University of Georgia, Tbilisi, Georgia*
¹⁵¹*Department of Physics, Technion, Israel Institute of Technology, Haifa, Israel*
¹⁵²*Raymond and Beverly Sackler School of Physics and Astronomy, Tel Aviv University, Tel Aviv, Israel*
¹⁵³*Department of Physics, Aristotle University of Thessaloniki, Thessaloniki, Greece*
¹⁵⁴*International Center for Elementary Particle Physics and Department of Physics, University of Tokyo, Tokyo, Japan*
¹⁵⁵*Department of Physics, Tokyo Institute of Technology, Tokyo, Japan*
¹⁵⁶*Department of Physics, University of Toronto, Toronto, Ontario, Canada*
^{157a}*TRIUMF, Vancouver, British Columbia, Canada*
^{157b}*Department of Physics and Astronomy, York University, Toronto, Ontario, Canada*
¹⁵⁸*Division of Physics and Tomonaga Center for the History of the Universe, Faculty of Pure and Applied Sciences, University of Tsukuba, Tsukuba, Japan*

- ¹⁵⁹*Department of Physics and Astronomy, Tufts University, Medford, Massachusetts, USA*
¹⁶⁰*Department of Physics and Astronomy, University of California Irvine, Irvine, California, USA*
¹⁶¹*University of Sharjah, Sharjah, United Arab Emirates*
¹⁶²*Department of Physics and Astronomy, University of Uppsala, Uppsala, Sweden*
¹⁶³*Department of Physics, University of Illinois, Urbana, Illinois, USA*
¹⁶⁴*Instituto de Física Corpuscular (IFIC), Centro Mixto Universidad de Valencia—CSIC, Valencia, Spain*
¹⁶⁵*Department of Physics, University of British Columbia, Vancouver, British Columbia, Canada*
¹⁶⁶*Department of Physics and Astronomy, University of Victoria, Victoria, British Columbia, Canada*
¹⁶⁷*Fakultät für Physik und Astronomie, Julius-Maximilians-Universität Würzburg, Würzburg, Germany*
¹⁶⁸*Department of Physics, University of Warwick, Coventry, United Kingdom*
¹⁶⁹*Waseda University, Tokyo, Japan*
¹⁷⁰*Department of Particle Physics and Astrophysics, Weizmann Institute of Science, Rehovot, Israel*
¹⁷¹*Department of Physics, University of Wisconsin, Madison, Wisconsin, USA*
¹⁷²*Fakultät für Mathematik und Naturwissenschaften, Fachgruppe Physik, Bergische Universität Wuppertal, Wuppertal, Germany*
¹⁷³*Department of Physics, Yale University, New Haven, Connecticut, USA*

^aDeceased.

^bAlso at Department of Physics, King's College London, London, United Kingdom.

^cAlso at Institute of Physics, Azerbaijan Academy of Sciences, Baku, Azerbaijan.

^dAlso at Lawrence Livermore National Laboratory, Livermore, USA.

^eAlso at TRIUMF, Vancouver, British Columbia, Canada.

^fAlso at Department of Physics, University of Thessaly, Greece.

^gAlso at An-Najah National University, Nablus, Palestine.

^hAlso at Department of Physics, University of Fribourg, Fribourg, Switzerland.

ⁱAlso at Department of Physics, Westmont College, Santa Barbara, USA.

^jAlso at Departament de Física de la Universitat Autònoma de Barcelona, Barcelona, Spain.

^kAlso at Affiliated with an institute covered by a cooperation agreement with CERN.

^lAlso at The Collaborative Innovation Center of Quantum Matter (CICQM), Beijing, China.

^mAlso at Università di Napoli Parthenope, Napoli, Italy.

ⁿAlso at Institute of Particle Physics (IPP), Canada.

^oAlso at University of Colorado Boulder, Department of Physics, Colorado, USA.

^pAlso at Borough of Manhattan Community College, City University of New York, New York, USA.

^qAlso at National Institute of Physics, University of the Philippines Diliman (Philippines), Philippines.

^rAlso at Department of Financial and Management Engineering, University of the Aegean, Chios, Greece.

^sAlso at Department of Physics, Stanford University, Stanford, California, USA.

^tAlso at Centro Studi e Ricerche Enrico Fermi, Italy.

^uAlso at Institutio Catalana de Recerca i Estudis Avancats, ICREA, Barcelona, Spain.

^vAlso at Technical University of Munich, Munich, Germany.

^wAlso at Yeditepe University, Physics Department, Istanbul, Türkiye.

^xAlso at Institute of Theoretical Physics, Ilia State University, Tbilisi, Georgia.

^yAlso at CERN, Geneva, Switzerland.

^zAlso at Center for Interdisciplinary Research and Innovation (CIRI-AUTH), Thessaloniki, Greece.

^{aa}Also at Hellenic Open University, Patras, Greece.

^{bb}Also at Center for High Energy Physics, Peking University, China.

^{cc}Also at Department of Physics, Stellenbosch University, South Africa.

^{dd}Also at Department of Physics, California State University, Sacramento, USA.

^{ee}Also at Département de Physique Nucléaire et Corpusculaire, Université de Genève, Genève, Switzerland.

^{ff}Also at Institut für Experimentalphysik, Universität Hamburg, Hamburg, Germany.

^{gg}Also at Institute for Nuclear Research and Nuclear Energy (INRNE) of the Bulgarian Academy of Sciences, Sofia, Bulgaria.

^{hh}Also at Washington College, Chestertown, Maryland, USA.

ⁱⁱAlso at Institute of Applied Physics, Mohammed VI Polytechnic University, Ben Guerir, Morocco.

^{jj}Also at Institute of Physics and Technology, Mongolian Academy of Sciences, Ulaanbaatar, Mongolia.